OULUN YLIOPISTO
UNIVERSITY of OULU

DEGREE PROGRAMME IN ELECTRICAL ENGINEERING

MASTER'S THESIS

EVALUATION OF THE AGGREGATE INTERFERENCE IN 2.4 GHz ISM BAND IN HOME, OFFICE AND HOSPITAL ENVIRONMENTS

Author	Theo D'Anna
Supervisor	Matti Hämäläinen
Second Examiner	Risto Vuohtoniemi

March 2015

D'Anna T. (2015) Evaluation of the Aggregate Interference in 2.4 GHz ISM Band in Home, Office and Hospital Environments. Communications Engineering, Programme in Electrical Engineering, University of Oulu, Oulu, Finland. Master's Thesis, 73 p.

ABSTRACT

In the last years, the wireless body area network (WBAN) research has grown considerably and the idea to apply WBAN to the medical and healthcare issues could materialize. A possible WBAN could exploit the ISM (industrial, scientific and medical) band, clustered around 2.4 GHz. The ISM band is just used by other communication systems and non-communication systems. These systems transmit signals, defined aggregate interference, that could hinder the WBAN communications.

In this thesis, the ISM band is investigated in order to understand if the amount of interference is too high to allow implementation of a new WBAN or if the coexistence between WBAN and the other systems is still possible.

The ISM band analyses are carried out using data collected in real-life measurements, in environments where a patient monitored by a WBAN could usually stay. Data was collected in an office and a home environments, situated in Florence, Italy, in "San Giuseppe" hospital located in Empoli, Italy and in Oulu University Hospital, situated in Oulu, Finland. In each location, data are collected during a week using a spectrum analyzer (SA). The information measured by the SA is the power, expressed in dBm.

In this work, a spectrum occupancy evaluation (SOE) has been developed to analyze the occupancy percentage of every frequency channel of the ISM band. The occupancy value is determined by a threshold, which divides the interference samples from the noise samples. In this work, the occupancy is evaluated using both a fixed threshold and a dynamic threshold, which value directly depends on the samples' values. The results achieved using fixed and dynamic thresholds are discussed and compared.

In addition, a time domain analysis has been carried out in order to know the amplitude, the time distribution and the size of the interference contributions. The time domain results allow to predict the interference behavior, making possible the extraction of a statistical interference modelling.

The final results of the analyses depend strongly on the measurement location, the time and the measurement equipment. However, in most cases, the occupancy value is below 10%. Hence, the amount of interference is not so high as to prevent the implementation of a new WBAN or to determine an added smartness to the WBAN.

Keywords: WBAN, ISM, interference, SOE, interference modelling.

D'Anna T. (2015) Kokonaishäiriön arviointi 2.4 GHz ISM-kaistalla koti-, toimisto- ja sairaalaympäristössä. Oulun yliopisto, Tietoliikennetekniikan osasto, sähkötekniikan koulutusohjelma. Diplomityö, 73 s.

TIIVISTELMÄ

Viime vuosina langattomien kehoverkkojen (WBAN) tutkimus on lisääntynyt huomattavasti ja ajatus WBAN:n soveltamisesta lääketieteen ja terveydenhoidon parissa on toteutumassa. Mahdollinen WBAN voisi hyödyntää ISM-taajuusaluetta (industrial, scientific and medical) 2.4 GHz:in alueella. ISM-kaistaa käytetään tiedonsiirron lisäksi myös muissa, ei-tietoliikennesovelluksissa. Nämä järjestelmät tuottavat radiotaajuista häiriötä, joka voi haitata WBAN-tietoliikennettä.

Tässä diplomityössä tutkitaan ISM-kaistalla esiintyvää radiotaajuista tehoa, jotta ymmärretään, onko häiriön määrä liian suuri sallimaan WBAN:n toteutuksen, vai onko WBAN:n ja muiden järjestelmien rinnakkaiselo mahdollista.

ISM-kaistan analyysit on tehty käyttäen dataa, joka on mitattu toimisto- ja kotiympäristöissä Firenzessä, Italiassa sekä San Giuseppen sairaalassa, Empolissa, Italiassa ja Oulun yliopistollisessa sairaalassa. Kussakin paikassa dataa kerättiin viikon ajan spektrianalysaattorilla (SA). Spektrianalysaattorilla mitattu data on radiokanavassa esiintyvien signaalien teho, a-joka on ilmaistu dBm:nä halutulla taajuusalueella.

Tässä työssä on tarkasteltu spektrin-käyttöastetta (SOE) ja analysoitu jokaista ISM-kaistan taajuuskanavan käyttötodennäköisyyttä. Käyttötodennäköisyys on määritelty kynnysarvolla, joka erottelee häiriönäytteet kohinanäytteistä. Tässä työssä spektrinkäyttöä arvioidaan käyttäen sekä kiinteää että dynaamista kynnysarvoa, jonka arvo muuttuu näytteiden arvon funktiona. Kiinteillä ja dynaamisilla kynnysarvoilla saatuja tuloksia analysoidaan ja verrataan keskenään.

Lisäksi työssä on toteutettu aika-alue -analyysi, jotta saadaan selville häiriötehon amplitudi, sen ajallinen hajonta sekä häiriövaikutusten laajuus. Aika-alueen tulokset mahdollistavat häiriön käyttäytymisen ennustamisen ja mahdollistavat tilastollisen häiriön mallintamisen.

Analyysien lopputulokset ovat vahvasti riippuvaisia mittausten sijainnista, ajankohdasta ja käytetystä mittauslaitteistosta. Useimmiten spektrin käyttöaste oli alle 10%. Näin ollen mitatuissa ympäristöissä häiriön määrä ei ole niin korkea, että se estäisi uuden WBAN:n toteutuksen.

Avainsanat: WBAN, ISM, häiriö, SOE, häiriön mallintaminen.

D'Anna T. (2015) Valutazione dell'Interferenza Aggregata nella Banda ISM a 2.4 GHz negli Ambienti Casa, Ufficio e Ospedale. Ingegneria delle Telecomunicazioni, Programma in Ingegneria Elettrica, Università di Oulu, Oulu, Finlandia. Tesi Magistrale, 73 p.

SOMMARIO

Negli ultimi anni, la ricerca relativa alla rete di sensori applicati al corpo umano (WBAN) è cresciuta notevolmente e l'idea di applicare WBAN nel campo medico potrebbe concretizzarsi. Una possibile WBAN potrebbe usufruire della banda ISM (industriale, scientifico e medico) a 2.4 GHz. La banda ISM è già utilizzata da altri sistemi di comunicazione e anche da sistemi di non-comunicazione. Questi sistemi trasmettono segnali, definiti interferenza aggregata, che potrebbero ostacolare le comunicazioni della WBAN.

In questa tesi è stata investigata la banda ISM al fine di capire se l'interferenza è troppo alta da permettere l'implementazione di una nuova WBAN o se la coesistenza tra WBAN e gli altri sistemi è ancora possibile.

Le analisi della banda ISM sono realizzate usando dati raccolti in campagne di misura, in ambienti dove un paziente, monitorato da una WBAN, potrebbe stare. I dati sono stati raccolti in un ufficio e in una casa, situati a Firenze, Italia, nell'ospedale "San Giuseppe" che si trova a Empoli, Italia e nell'Ospedale Universitario di Oulu, situato ad Oulu, Finlandia. Le campagne di misura sono durate una settimana ed è stato usato un analizzatore di spettro (SA). L'informazione raccolta dall'analizzatore di spettro è la potenza, espressa in dBm.

In questo elaborato è stata sviluppata una valutazione dell'occupazione spettrale (SOE) per analizzare la percentuale di occupazione di ogni canale di frequenza della banda ISM. Il valore di occupazione dipende da una soglia, che divide i campioni di interferenza dai campioni di rumore. In questo lavoro, l'occupazione è valutata sia con una soglia fissa che con una soglia dinamica, il cui valore dipende direttamente dall'ampiezza dei campioni. I risultati ottenuti con la soglia fissa e dinamica sono stati analizzati e confrontati.

In questa tesi è stata realizzata anche un'analisi nel dominio temporale al fine di conoscere l'ampiezza, la distribuzione temporale e la dimensione dei contributi di interferenza. I risultati ottenuti dalle analisi nel dominio temporale permettono di predire le caratteristiche dell'interferenza, rendendo possibile l'estrazione di un modello statistico di interferenza.

I risultati finali delle analisi dipendono fortemente dal luogo in cui sono state realizzate le misurazioni, dal tempo e dall'apparecchio di misura. Tuttavia, nella maggior parte dei casi, i valori dell'occupazione sono minori del 10%. Quindi, l'interferenza non è così alta da impedire l'implementazione di una nuova WBAN o da determinare l'aggiunta di intelligenza alla WBAN.

Parole chiave: WBAN, ISM, interferenza, SOE, modello di interferenza.

TABLE OF CONTENTS

PREFACE

The research for this thesis has been carried out in the Centre for Wireless Communications (CWC) at the University of Oulu, in Oulu, Finland. This work springs by the collaboration between CWC and DINFO (Dipartimento di Ingegneria dell'Informazione), Department of Information Engineering of the University of Florence, in Florence, Italy.

I would like to thank my Italian supervisor Dr. Lorenzo Mucchi for the interest that he has always shown in my work and for giving me the possibility to make this amazing experience in Oulu. I acknowledge Ing. Alessio Carpini for his availability and his help.

I would like to thank Prof. Jari Iinatti for accepting me in CWC and Prof. Risto Vuohtoniemi for reviewing this thesis. I'm grateful to Ing. Hasnain Virk for his precious instructions, for encouraging me and for telling me the words which I needed. I really hope to see you again, my friend! I acknowledge Kirsi Ojutkangas for the help at the beginning of this experience, for her availability and kindness. I would like to thank my office mates Samad, Praneeth, Ahad and all the CWC staff, for making the working environment excellent and stimulant.

I would like to thank Alessandro Pagani, Claudio Ferreira Dias and Antti Partanen for their company and for making this experience in Oulu unforgettable. Thank you friends! My gratitude goes especially to Antti for translating the abstract in Finnish.

Finally, I would like to thank Dr. Matti Hämäläinen my supervisor, my guide, my mentor. Without him it would have not been possible to finish this work.

Leaving Oulu is one of the most difficult things that I have never done in my life, I will never forget!

Oulu, March 2015

Theo D'Anna

LIST OF SYMBOLS AND ABBREVIATIONS

ACL	asynchronous connection oriented
A/D	analog to digital
AES	advanced encryption standard
AP	access point
ARQ	automatic repeat request scheme
BIC	Bayesian information criterion
BS	base station
BSS	basic service set
BT	Bluetooth
CCK	complementary code keying
CDF	cumulative distribution function
CRS	cognitive radio system
CSMA/CA	carrier sense multiple access with collision avoidance paradigm
CSRR	clean sample rejection rate
DCF	distributed coordination function
DS	distribution system
DSSS	direct sequence spread spectrum
ECG	electrocardiogram signal
ED	energy detection
EIRP	equivalent isotropic radiated power
ESS	extended service set
FBO	frequency band occupancy
FCME	forward consecutive mean excision algorithm
FCO	frequency channel occupancy
FEC	forward error correction
FFD	full function device
FHSS	frequency hopping spread spectrum
GEV	Generalized extreme value distribution
GFSK	Gaussian frequency-shift keying
GSM	global system for mobile communications
IBSS	independent BSS
ICT	information and communication technology
IEEE	the Institute of Electrical and Electronics Engineers
ISM	industrial, scientific and medical band
ISO/OSI	International Standards Organization Open Systems Interconnection
ITU-R	the International Telecommunication Union Radiocommunication sector
LAN	local area network
L2CAP	logical link control and adaptation protocol
MAC	medium access control
med-FCME	median FCME
MIMO	multiple-input multiple-output
MRI	magnetic resonance imaging

OFDM	orthogonal frequency-division multiplexing
PAN	personal area network
PCF	point coordination function
PDF	probability density function
PHY	physical layer
QOS	quality of service
RFD	reduced function device
SA	spectrum analyzer
SCO	synchronous connection oriented
SNR	signal-to-noise ratio
SOE	spectrum occupancy evaluation
SRO	spectrum resource occupancy
TDD	time division duplex
UMTS	universal mobile telecommunication system
WBAN	wireless body area network
WiFi	wireless fidelity
WLAN	wireless local area network
WPAN	wireless personal area network

B_{S}	ISM bandwidth
c	frequency index
D	binary matrix
D(*i*,*c*)	(*i*,*c*) element of matrix **D**
FBO_{τ}	FBO computed using M_{τ} sweeps
FBO_{i}	FBO of the i-th sweep
FCO_{c}	FCO of the c-th channel
i	sweep index
k	shape parameter
l	cluster index
$\hat{L}$	maximized value of likelihood function
M	number of sweeps
M_{τ}	number of sweeps collected during τ
N	number of frequency domain samples
N_{λ}	number of thresholds
N_{B}	total number of samples in the band, collected during τ
N_{C}	total number of channel samples collected during τ
N_{Ch}	maximum number of channels
N_{O}	number of measurements with level greater than the threshold
N_{OB}	number of samples in the band with level greater than the threshold
N_{OC}	number of channel samples with level greater than the threshold
N_{OR}	samples number in any channel with level greater than the threshold

N_{R}	total number of samples taken from all the channels during τ
p	value defining percentile
$P_{(i,c)}$	power sample
PFA_{DES}	desired clean sample rejection rate
Q	size of the initial data set
R	statistical distribution in analysis
T_{Bobs}	band observation time
$T_{\mathrm{I,C}}$	continuous interarrival time
$T_{\mathrm{I,D}}$	discrete interarrival time
T_{M}	sample measurement time
T_{O}	occupancy time
T_{Obs}	observation time
T_{proc}	processing time
T_{R}	revisit time or sweep time
T_{T}	duration of monitoring
v	size of the cluster size, interarrival time and cluster amplitude vectors
w	number of the statistical model parameters
x_{c}	sample amplitude
y	cluster size, interarrival time and cluster amplitude vectors
z	number of samples below the threshold that divide two consecutive clusters
α_{i}	threshold achieved through med-FCME algorithm
γ	fixed detection threshold
γ_{i}	dynamic detection threshold
θ	threshold parameter
λ_{CME}	threshold for consecutive mean excision
λ_{h}	threshold iteratively calculated through FCME algorithm
μ	location parameter
$\hat{\xi}$	statistical model parameters
σ	scale parameter
τ	integration time

1. INTRODUCTION

Nowadays, the necessity to implement WBANs (wireless body area networks) for healthcare applications is very strong. In fact, the aim of the healthcare sector is to monitor the patients' vital parameters through sensors, without constraining the patients to lie in a bed of a hospital ward. Patients could remain in their homes, could keep on working in their office or could stay in the reception area of the hospital while the vital parameters are monitored by the sensors and transmitted to the electronic patient record through a wireless link.

The medical ICT (information and communication technology) researchers designate the ISM band as a possible band for WBANs used in healthcare applications. The ISM band is particularly overcrowded: communication protocols such as Bluetooth (BT), Zigbee and WLAN (wireless local area network) and also non-communication systems such as microwave ovens use this band. All the systems mentioned above produce interference signals that can disturb the transmission of a hypothetic WBAN. Hence, an investigation of the ISM band is necessary in order to analyze its behavior and to identify the spectral resources that it still offers.

The ISM band analyses are carried out considering data collected in real-life measurements, in environments where patients, monitored by a WBAN, could stay such as home, office or hospital. In this work, the spectrum occupancy evaluation is carried out in order to define the occupancy percentage of the ISM band. The International Telecommunication Union Radiocommunication sector (ITU-R) describes the spectrum occupancy measurements procedures in [1–3]. The spectrum occupancy evaluation is studied, e.g., in [4–11]. ISM band is analyzed also in time domain to define the time trend of the interference contributions. Moreover, a statistical interference model can be extracted by the time domain results. The interference modelling can be used to predict the interference behavior in the environments considered, removing the necessity of new measurement campaigns. Interference modelling is analyzed, e.g., in [12–16]. The ISM band behavior strongly influences the WBAN design. WBAN for healthcare applications needs frequency channels free from interference. If high amount of interference is detected in the ISM band, the implementation of a cognitive radio system (CRS) is necessary. CRS devices are able to know the amount of interference in every frequencies of the ISM band and to transmit using the frequency that presents the lowest value of interference. Otherwise, if the amount of interference in the ISM band is low, in all the frequency channels considered, the CRS is not necessary and the WBAN can use every frequency for transmitting. Obviously, the implementation of a CRS makes the WBAN smart, more complicated and very expensive.

This thesis is organized as follows: In Chapter 2, an overview of WBAN and the protocols that exploit the ISM band is given. Chapter 3 analyzes the theoretical concepts and the algorithms related to the spectrum occupancy evaluation. Chapter 4 describes the environments on which the measurement campaigns were carried out and the measurement equipment used. In Chapter 5, the spectrum occupancy results are discussed. In Chapter 6, the time domain analysis results and the interference modelling are described. Chapter 7 reports a discussion about the results achieved in this work. Chapter 8 summarizes the most important steps carried out in the thesis.

2. STANDARDS IN ISM BAND

In this chapter, the standards that utilize the ISM band are described. The ISM band is available worldwide. It is an unlicensed frequency band, hence it can be freely used, but communication equipments operating in this band have to transmit with very low power to limit the interferences with other devices. Maximum equivalent isotropic radiated power (EIRP) is 36 dBm [17].

There are three ISM bands globally defined [17]:

- 900 MHz band, [902-928 MHz].
- 2.4 GHz band, [2400-2485 MHz].
- 5.8 GHz band, [5725-5875 MHz].

The medical ICT research, carried out until now, designates the ISM band clustered around 2.4 GHz, as the band of a possible WBAN for healthcare applications. In this range of frequencies coexist non-communication systems like microwave ovens, microwave diathermy and communication standards like WLAN, Bluetooth, Zigbee and Cordless phones [18]. The measurements considered in this work are carried out in the ISM band in order to examine the possible interference problem caused by the existing systems mentioned above and for understanding if the ISM band still offers resources for the implementation of a new WBAN.

This chapter is organized as follows: in Section 2.1, a WBAN overview is given. In Section 2.2, the standards related to WLAN are described. Section 2.3 examines Bluetooth network. Section 2.4 analyzes the Zigbee protocol.

2.1. Wireless body area network

WBAN is a sensor network technology which can be used in several domains such as fitness management, entertainment, security, military and medical issues [19]. In medical case, the sensor nodes are applied to the human body of the patients to monitor several physiological parameters such as heartbeat, body temperature and blood pressure.

In Figure 1, an example of WBAN sensor structure is shown [20]. The sensing unit detects the analog signals and converts the analog signals in digital signals through the A/D (analog to digital) converter. The processor unit performs filtering and amplification operations. The storage unit stores the signals. The location finding system identifies the sensor position. The actuator converts an electrical signal to a physical action, related to the sensor's application field. The communication unit, formed by the transceiver and the antenna, transmits data to a central node, called as a sink node, coordinator node or hub. The power unit and the power generator provide the power to all these components. [19], [21]

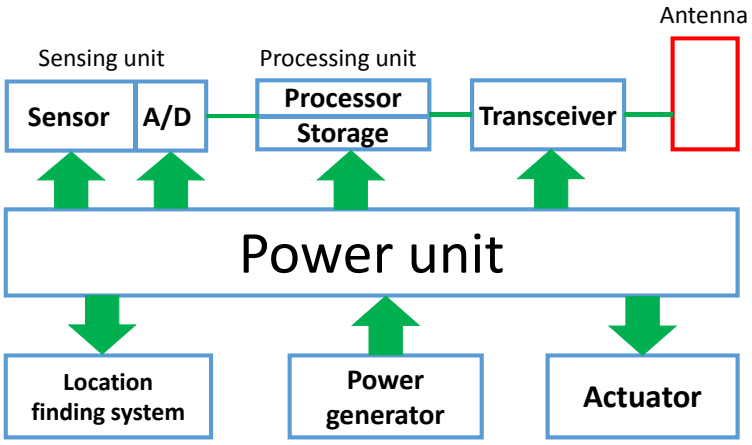

Figure 1. Sensor structure.

The coordinator node transmits data to a backbone network through a wireless link. The illustration of a WBAN is shown in Figure 2. The wireless link can be supported by WLAN, global system for mobile communication (GSM), universal mobile telecommunication system (UMTS), etc [22].

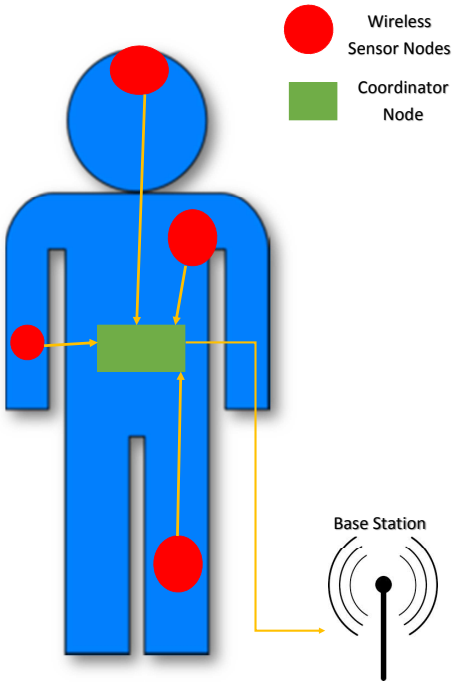

Figure 2. Graphical description of a WBAN.

Figure 2 shows that typical WBAN is not node-dense. There is only a little amount of nodes, placed in precise locations of a human body. Nodes have to be inexpensive, small and energy efficient [19].

WBAN supports peer-to-peer and infrastructure architectures. In the first case, all nodes can communicate with all other nodes and the nodes are equipotent. In an infrastructure network, all the communications between nodes have to pass through an access point (AP) or a base station (BS) [19].

The Institute of Electrical and Electronics Engineers (IEEE) developed a standard for WBANs in 2012 [19]. This standard, called IEEE 802.15.6, defines the physical layer (PHY) and the medium access control (MAC) protocol. The utilization of IEEE 802.15.6 is not obligatory and other protocols can be used for implementing a WBAN.

Short range wireless technologies, such as Zigbee and Bluetooth, can be implemented for WBAN applications. In fact, Zigbee and Bluetooth support communications between sensors that provide minimum power consumption. Moreover, Zigbee and Bluetooth guarantee that sensor batteries had a long life [19].

2.2. Wireless local area network

WLAN is a network that connects devices through a wireless link in restricted environments, such as office or house. A WLAN can be used concurrently by a large number of nodes and it guarantees wireless communications with high throughput.

IEEE 802.11 protocols, that form the 802.11 suite, describe and standardize the WLAN features. This suite supports four different physical layer types such as DSSS (direct sequence spread spectrum), FHSS (frequency hopping spread spectrum), infrared and OFDM (orthogonal frequency-division multiplexing) [17]. These standards define also a medium access control layer common to all these physical layers.

In a WLAN there are several kinds of elements:

- Station: Any device characterized by an IEEE 802.11 MAC and physical layer.
- Basic service set (BSS): A set of stations managed by a coordination function (i.e., logic function that manages access to the physical channel).
- Distribution system (DS): System that interconnects a set of BSS and integrated local area networks (LANs) to implement an extended service set (ESS).
- Access point: Station that allows associated station to access the distribution system.
- ESS: A set of interconnected BSSs and integrated LANs.

The BSS can be infrastructure BSS or independent BSS (IBSS). In the first case, an infrastructure network is achieved. In the other case, an ad hoc network is obtained [17]. In Figure 3, an illustration of an infrastructure and an ad hoc network is shown.

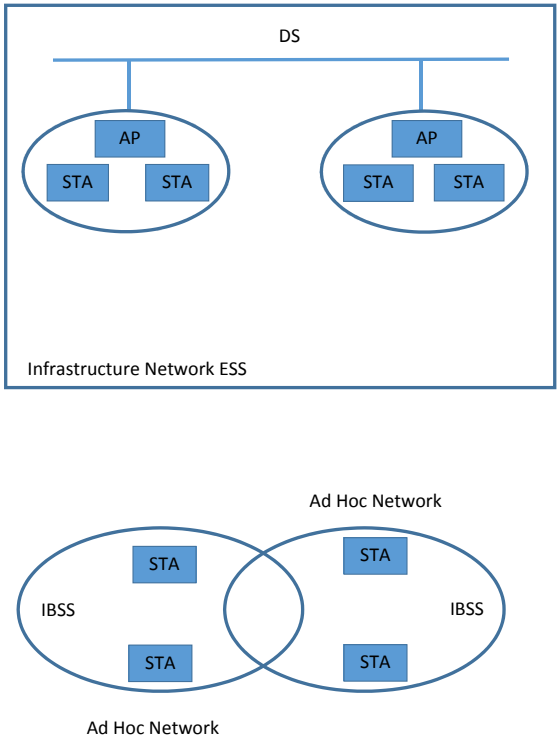

Figure 3. On the top: infrastructure network. On the bottom: ad hoc network.

The access to the physical channel is regulated through the coordination function. There are two types of coordination functions [17]:

- Distributed coordination function (DCF).
- Point coordination function (PCF).

The DCF can be used both in an infrastructure BSS and in a IBSS and it allows a coordination among stations without a central node. This function is based on the carrier sense multiple access with collision avoidance paradigm (CSMA/CA). PCF can be used only in an infrastructure BSS, the channel access is managed by a central node, called point coordinator that manages the transmissions of all the stations. [17]

The IEEE 802.11 protocols define management operations such as [17]:

- Scanning.
- Authentication.
- Association.
- Power management.
- Synchronization.

The scanning is an operation made by the stations to connect themselves to a BSS. There are two kinds of scanning: passive or active. In the first case, the station hears all the BSSs channels available and stores the packages ("beacon") received from them. In the second case, the station transmits continuously packages to urge the transmission of the beacon by the BSS. At the end of this phase, the station creates a database with an entry for each BSS. [17]

During the association, the station and the AP are connected to each other. Next, the station is authenticated by the access point. There are several kinds of authentication system such as open system authentication and shared key authentication. [17]

The 802.11 suite is composed by protocols that principally use two bands: the 2.4 GHz band and the 5 GHz band. The protocols that utilize the 2.4 GHz band are [23], [24]:

- IEEE 802.11-1997.
- IEEE 802.11b.
- IEEE 802.11g.
- IEEE 802.11n.

The bandwidth utilized by these standards is divided in 14 overlapping channels. The channels related on IEEE 802.11-1997 protocol are shown in Figure 4 [23]. Subsequently, the features of the above mentioned protocols are listed, highlighting their frequencial allocations.

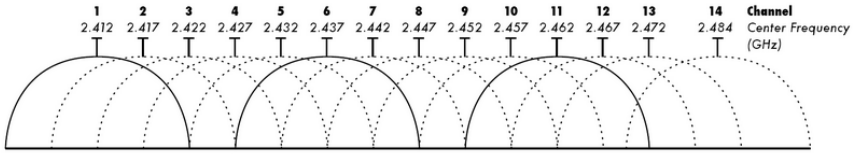

Figure 4. 14 overlapping channels in the ISM band.

IEEE 802.11-1997 is the first protocol of the suite. It specifies two data rates of 1 and 2 Mbit/s. It supports three physical layer technologies: infrared working at 1 Mbit/s, FHSS working at 1 Mbit/s or 2 Mbit/s, and DSSS operating at 1 Mbit/s or 2 Mbit/s. IEEE 802.11-1997 implements a forward error correction (FEC). This standard is now obsolete. [17], [23], [24]

In Figure 5, the non-overlapping channels related to this protocol (i.e., number 1, 6, 11 and 14) are shown. In the figure, the number of the channels and center frequencies are indicated [23].

Different WLANs could coexist in the same environment, but each network has to work on a different non-overlapping channel. In this way, the interference between WLANs will be reduced to minimum values. For this standard, the channel bandwidth is 22 MHz. [17], [23], [24]

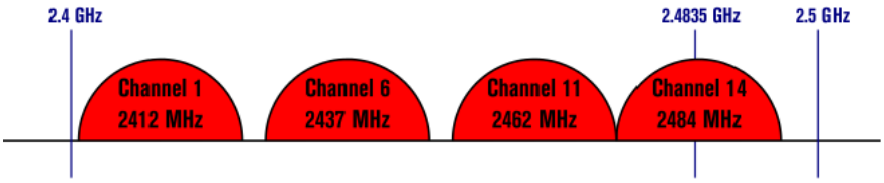

Figure 5. Non-overlapping channels of IEEE 802.11-1997 and IEEE 802.11b protocol.

IEEE 802.11b allows a data rate of 11 Mbit/s. IEEE 802.11b is based on complementary code keying (CCK). These codes have immunity to multipath and ensure high throughput. IEEE 802.11b has the same channels' arrangement than IEEE 802.11-1997 (Figure 5). The channels have bandwidth of 22 MHz. [17], [23], [24]

IEEE 802.11g was ratified in 2003. It supports the OFDM. This technique allows a data rate of 54 Mbit/s. IEEE 802.11g supports also the DSSS technique and it is compatible with the standards mentioned above. IEEE 802.11g presents three non-overlapping channels. The channel bandwidth is 20 MHz, but only 16.25 MHz are used by the OFDM sub-carries (Figure 6). [17], [23], [24]

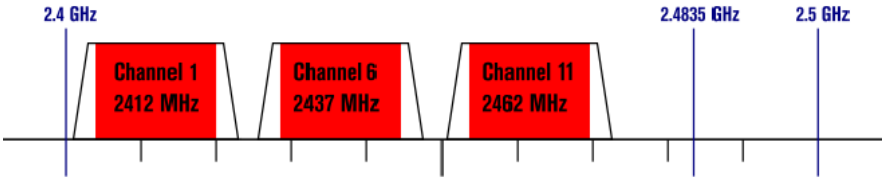

Figure 6. Non-overlapping channels of IEEE 802.11g.

IEEE 802.11n supports OFDM and it improves IEEE 802.11g adding multiple-input multiple-output antennas (MIMO). This protocol supports a data rate that can reach 600 Mbit/s. Moreover, IEEE 802.11n supports the quality of service (QOS) in the MAC level. There is a non-overlapping channel with a bandwidth of 40 MHz, but only 33.75 MHz are used by the OFDM sub-carries (Figure 7). [17], [23], [24]

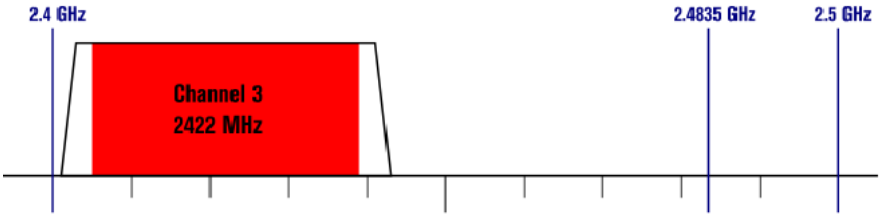

Figure 7. Non-overlapping channel of IEEE 802.11n.

2.3. Bluetooth

Bluetooth is a wireless standard used to implement WPAN (wireless personal area network). It operates also in the ISM band. Bluetooth is used for transmitting data and voice in real time in ad hoc type networks. It is utilized for connecting peripheral devices (e.g., joystick, loudspeaker, printer). Bluetooth ensures low power consumption, but data rate is very low and the application range is limited. [25], [26] More details about power consumption, data rate and application range are given in the final part of this section.

A Bluetooth network is formed by two units: the master and the slave. There are two kinds of network [26]:

- Piconet.
- Scatternet.

The first one is a small ad hoc network formed by, at most, 8 simultaneously active devices (1 master and 7 slaves). The piconet can be monoslave (1 master and one slave) or multislave (1 master and several slaves) [26].

Scatternet is achieved through the combination of piconets that coexist and operate in the same zone. In a Scatternet, one device in each piconet (either a master or a slave) acts like a bridge between piconets [26].

The protocol that standardizes Bluetooth is called IEEE 802.15.1. It defines the Bluetooth protocol stack and describes the layers that form this stack. The stack is represented in Figure 8 [27].

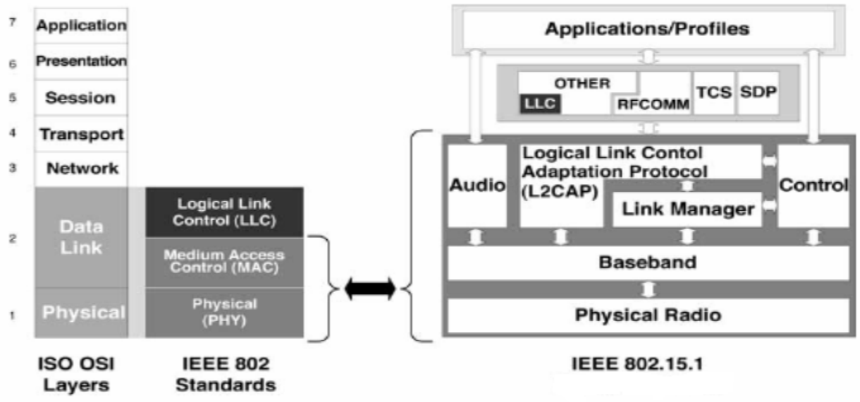

Figure 8. On the left: ISO/OSI (International Standards Organization Open Systems Interconnection) stack, on the right: Bluetooth stack.

Bluetooth radio uses 2-GFSK (Gaussian frequency-shift keying) modulation and the maximum power in transmission is 20 dBm (value related to the first Bluetooth version) [26].

Baseband defines, as transmission technique, the FHSS combined with the time division duplex (TDD). FHSS technique divides the whole band clustered around 2.4 GHz in 79 channels of 1 MHz (the total band is 80 MHz). Every device uses, at each

temporal slot (the slot duration is 0.625 ms), a frequency channel. The transmission frequency depends on a pseudo-random frequency hopping code. The transmitting frequency changes 1600 times in a second. In a piconet, the master transmits in the even-numbered slots and the slaves transmit in the odd-numbered slots. The master chooses the hopping sequence and the slaves must synchronize themselves to this sequence. [25]

Baseband layer defines also the communication rules between master and slave. There are two kinds of connections between master and slave [26]:

- Synchronous connection oriented (SCO).
- Asynchronous connection oriented (ACL).

The first one is a symmetric, point-to-point connection. It provides guaranteed bandwidth, hence, it is utilized for real-time traffic, such as voice and music. SCO can reach 64 kbit/s (value related to the first Bluetooth version) [26].

ACL is a point to multipoint connection. It can be symmetric or asymmetric and it supports data traffic. The maximum data rate is 721 kbit/s in asymmetric modality or 432.6 kbit/s in symmetric modality (values related to the first Bluetooth version) [26].

Baseband layer manages also the error correction that can be FEC or automatic repeat request scheme (ARQ) [26]. Baseband describes the modes on which a Bluetooth device can be during a connection [26]:

- Active mode: The unit is active in the channel, it can transmit or receive packages.
- Sniff mode: The unit sleeps for a predetermined number of slots, after those it wakes up for transmitting its packages in a predetermined slot. It is a power-saving mode.
- Hold mode: The unit can't transmit ACL data, but only SCO data. It is a power-saving mode.
- Park mode: The unit returns its active address, but it continues to be synchronized to the net. It is a power-saving mode.

Link Manager Control defines link setup, authentication and link management. **L2CAP** (logical link control and adaptation protocol) provides packages segmentation. Moreover it manages connection-oriented and connectionless data services. [26]

Bluetooth is divided into three classes, class 1 represents the first Bluetooth version and class 3 is the highest Bluetooth evolution in terms of transmission power. The features of these classes are given in Table 2. [19], [28]

Table 2. Bluetooth classes

Class	Max. power	Range	Data rate
Class 1	20 dBm	100 meters	1 Mbps
Class 2	4 dBm	10 meters	3 Mbps
Class 3	0 dBm	1 meters	24 Mbps

2.4. Zigbee

Zigbee technology is used to implement personal area networks. Zigbee forms wireless mesh networks, where the nodes have low power consumption, long battery life, low data rate (250 kbit/s) and limited range. This technology is standardized by the protocol IEEE 802.15.4 that defines the PHY layer and the MAC layer. [19], [28], [29]

Physical layer: Zigbee uses the ISM band clustered around 2.4 GHz. The band is divided in 16 channels, with each channel spaced 5 MHz apart. Every channel uses only 2 MHz of bandwidth (Figure 9). The transmission technology supported is DSSS. [29]

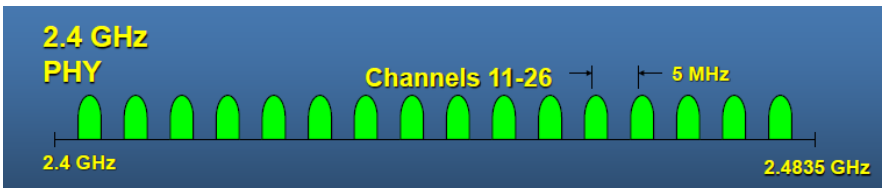

Figure 9. Zigbee channels.

MAC layer defines CSMA/CA channel access and the advanced encryption standard (AES) security system [29]. In Zigbee there are two different device types:

- Full function device (FFD).
- Reduced function device (RFD).

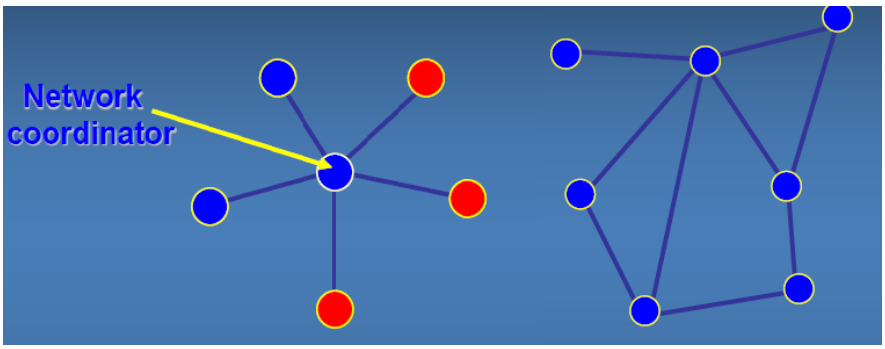

Figure 10. On the left: star topology, on the right: peer-to-peer topology. In blue: FFD, in red: RFD.

The FFD can fill the role of device, coordinator and PAN (personal area network) coordinator. The RFD can only fill the role of device. Zigbee supports two kinds of network topology: star topology and peer-to-peer topology (Figure 10). These topologies could be combined [29].

3. SPECTRUM OCCUPANCY THEORY

This chapter covers all theoretical concepts on which this thesis is based on. In the first part, the most important parameter definitions that will be used in the rest of this project are given. Next, in Section 3.2, the steps that allow to evaluate mathematically these parameters are analyzed and subsequently, in Section 3.3, the algorithms that implement these steps are described.

3.1. Definitions

The following section reports the definitions of the parameters related to the topics discussed in this thesis. These parameters are utilized to analyze the spectrum and to understand if it offers already resources (in time and frequency domains) for the implementation of new networks.

What matters most is the spectrum occupancy evaluation that could be done by computing three parameters:

1. Frequency channel occupancy (FCO).
2. Frequency band occupancy (FBO).
3. Spectrum resource occupancy (SRO).

Definitions of these parameters are closely related to the definitions of the other parameters, listed below:

Duration of monitoring (T_{T}): Temporal duration of occupancy measurements. Usually the monitoring durations are 24 h [2].

Sample measurement time (T_{M}): Temporal duration of one channel or frequency point measurement [2].

Observation time (T_{Obs}): Time required to make measurements on one channel, it includes also the time necessary for the channel processing overhead, due to, for example, data storage ($T_{\mathrm{Obs}} = T_{\mathrm{M}} +$ time for processing overhead) [2].

Revisit time or sweep time (T_{R}): Time required to monitor all the channels [2].

Occupancy time (T_{O}): Time interval on which the channel's measured energy level has got a value higher than a threshold. In a multiple channels analysis, a particular channel is considered. After a revisit time, this channel will be observed again if the channel is still occupied, it is assumed that the channel was occupied also during the time in between the two measurements [2]. It can be calculated by

$$T_{\mathrm{O}} = N_{\mathrm{O}} \cdot T_{\mathrm{R}}, \tag{1}$$

where N_{O} is number of measurements with level higher than a threshold.

Integration time (τ): In a particular moment, a channel can be occupied or not, hence the temporary occupancy of a channel can only be 0% or 100%. All occupancy values calculated must be averaged over a certain time period that is called integration time. The integration time can be 5 min, 15 min, one hour, one day, or the whole monitoring duration [2].

Maximum number of channels (N_{Ch}): Maximum number of channels which can be monitored during the revisit time [2].

Band observation time (T_{Bobs}): Time required to make measurements on all the channels. T_{Bobs} includes also the time necessary for the channels processing overhead (T_{proc}), due to, for example, data storage (T_{Bobs} = $T_{\mathrm{R}} + T_{\mathrm{proc}}$). T_{Bobs} can be also calculated as

$$T_{\mathrm{Bobs}} = N_{\mathrm{Ch}} \cdot T_{\mathrm{Obs}}. \tag{2}$$

Threshold: Power value that establishes if a channel can be considered occupied or not. It may be a fixed or a variable level. The occupancy value is strongly influenced by the choice of the threshold [2].

Now it is possible to define FCO, FBO and SRO.

Frequency channel occupancy: For one channel, the FCO is computed as

$$FCO = \frac{T_{\mathrm{O}}}{\tau}. \tag{3}$$

If the revisit time is constant, the FCO becomes

$$FCO = \frac{N_{\mathrm{OC}}}{N_{\mathrm{C}}}, \tag{4}$$

where N_{OC} is the number of channel samples with energy level greater than the threshold and N_{C} is the total number of channel samples collected during the integration time [2].

For evaluating the frequency channel occupancy, the bandwidth considered by the telecommunication system is divided in channels. Each channel is characterized by a certain number of samples. A channel is defined occupied if the channel samples that exceed the noise threshold are more than 50%. This proceeding is applied to all the channels, for computing every channel occupancy. [30]

Frequency band occupancy is useful to understand the amount of bandwidth occupied. Assuming the measurement time of each sample is equal, the FBO is computed by

$$FBO = \frac{N_{\mathrm{OB}}}{N_{\mathrm{B}}}, \tag{5}$$

where N_{OB} is number of the samples in the band with energy level greater than the threshold and N_{B} is total number of samples in the band collected during the integration time [2].

Spectrum resource occupancy: SRO is the averaged FCO of multiple channels. Precisely it is the ratio of the number of channels occupied to the total number of channels in a whole frequency band. The SRO is calculated as

$$SRO = \frac{N_{\mathrm{OR}}}{N_{\mathrm{R}}}, \tag{6}$$

where N_{OR} is number of samples in any channel with energy level greater than the threshold and N_{R} is the total number of samples taken from all the channels during the integration time. When only one channel is measured, the SRO is equal to the FCO [2].

3.2. Spectrum occupancy evaluation

The following section describes the most important steps for estimating the spectrum occupancy, i.e., FCO, FBO, SRO. The main steps are:

1. Energy detection (ED).
2. Threshold selection.
3. Spectrum occupancy computation.

3.2.1. Energy detection

Energy detection is a spectrum sensing mechanism which was chosen because it is simple and easier to implement than the other spectrum sensing mechanisms like cyclostationary features method, wavelet decomposition, and matched filtering [31]. On the other hand, these more complex mechanisms are able to detect various features of the signal (e.g., cyclostationarity is able to differentiate single carrier and multicarrier systems), instead ED is able to consider only magnitude, and loses phase information of the signal. [5], [18]

Energy detection process provides a matrix of power samples, size of [M]x[N], where M is number of sweeps and N is number of frequency domain samples. After that, each power sample is compared to a threshold to asses if signals are present or if only noise was received.

3.2.2. Threshold selection

One of the most important factors for evaluating the spectrum occupancy is the threshold. The threshold value has to be low enough for detecting all signals, but if it is too low, the noise floor can be wrongly classified as a signal [2].

There are principally two kinds of threshold:

1. Pre-set or fixed threshold.
2. Dynamic threshold.

Fixed threshold

In this case, the threshold has got a fixed value that remains constant through the whole duration of data analysis. All the power values collected are compared to the same fixed threshold γ. The threshold depends on :

1. The minimum wanted received power.
2. Required signal-to-noise ratio (SNR).

Hence, in this case, the required signal-to-noise ratio of the system and the minimum wanted received power have to be specified. [2] The system designer sets the fixed threshold in function of these parameters. Details about the fixed threshold setting are reported in Chapter 5.

Dynamic threshold

An important problem could be the noise uncertainty. In fact, it may determine a phenomena called "SNR wall", which causes the failure detection of a weak signal. Noise uncertainty is caused by thermal noise level variations due to ambient noise and variable temperature (and also due to galactic noise, atmospheric noise, noise caused by accidental radiation from electrical and electronic equipment, electrical machinery and power transmission lines). The approach based on a fixed threshold is more fragile against the noise than the analysis based on a dynamic threshold. [11] There are several algorithms to calculate dynamic thresholds, but in this work only two of them are considered [11], [32–34]:

1. Forward consecutive mean excision (FCME) threshold.
2. Median-FCME (med-FCME) threshold.

FCME threshold It is possible to compute a dynamic threshold using the FCME algorithm. FCME sets a threshold following these steps:

STEP 1: Desired clean sample rejection rate PFA_{DES} is selected. PFA_{DES} is defined as a function of the clean sample rejection rate (CSRR). It represents the number of noise-only samples wrongly classified by the algorithm as outliers having signal components. Only a small CSRR value, i.e., false alarm is tolerated. For example, CSRR can be 5%, which means that PFA_{DES} = 0.05. [11], [32]

STEP 2: Threshold for consecutive mean excision (λ_{CME}) is calculated by

$$\lambda_{\mathrm{CME}} = -\ln(PFA_{\mathrm{DES}}). \tag{7}$$

If PFA_{DES} = 0.05, λ_{CME} = 2.99. [32], [33]

STEP 3: The FCME algorithm sorts the frequency domain samples in an ascending order as a function of their energies. The number of frequency domain samples is N. An initial set formed by the least powerful samples, i.e., the samples which are free of interference, is considered. A large initial data set determines a lower computational complexity of the algorithm, because less iterations are needed, but it increases the possibility that the initial data set is not free of interference [11]. A small initial data set may determine a too small initial threshold and it is possible that the algorithm doesn't converge. Usually, the size of the initial set is 10% of all the samples. The size of this set is *Q*. [32–34]

STEP 4: Calculate first threshold

$$\lambda_{\mathrm{h}} = \frac{1}{Q}\sum_{c=1}^{Q} \mid x_c \mid^2 \cdot \lambda_{\mathrm{CME}}, \tag{8}$$

where x_c is the *c*-th sample and $\frac{1}{Q}\sum_{c=1}^{Q} \mid x_c \mid^2$ is the average sample mean of the initial data set. [32–34]

STEP 5: Add samples x_c, where *c* = *Q*+1,..., *N* to data set, composed by Q samples, if $\mid x_c \mid^2 < \lambda_{\mathrm{h}}$. This new data set is used for evaluating the new threshold according to (8). Hence the FCME iteratively calculates a new mean and a new threshold until there

are no new samples below the threshold. [32], [33] If the number of noise-only samples is scarce, the noise floor could be too elevated, hence to achieve an efficient algorithm, a large amount of noise-only samples is necessary [11]. The system designers set the value of PFA_{DES}. If PFA_{DES} is low, λ_{CME} is high and λ_{h} is high. Otherwise if PFA_{DES} is high, λ_{CME} is low and λ_{h} is low. If the threshold is too high, it is possible to fail the detection of important interference contributions, otherwise if the threshold is too low, noise can be wrongly classified as interference. [33] The graphical explanation of FCME algorithm is presented in Figure 11. The circle boxes represent the selection steps, the rhombus boxes depict the computation steps and the square boxes figure the conditional instructions.

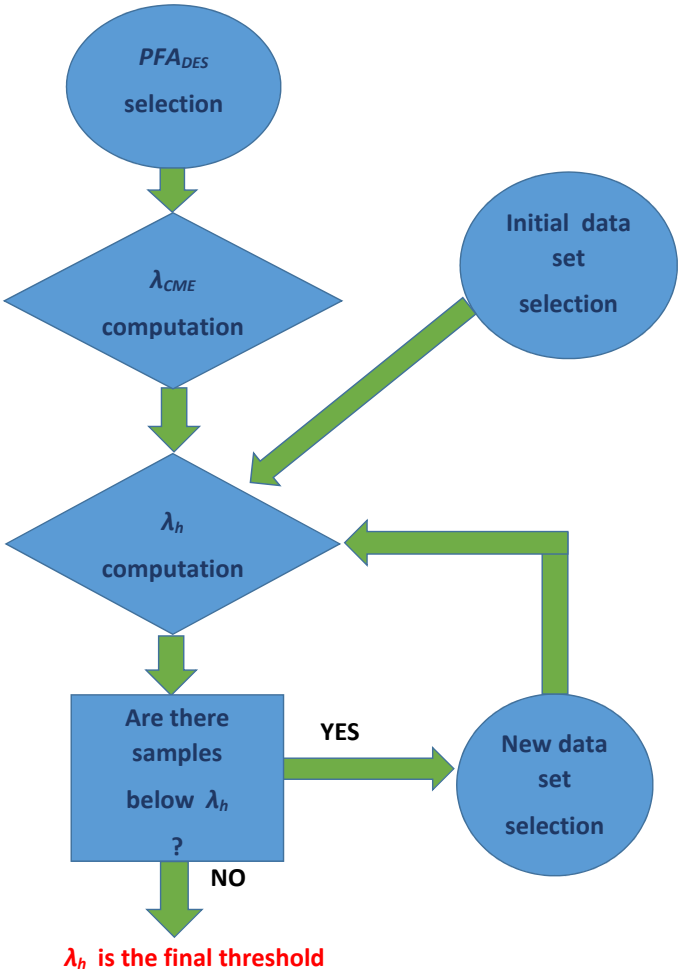

Figure 11. FCME algorithm scheme.

Med-FCME threshold Med-FCME is based on the FCME principles and it can be considered as an improvement of that. A median filter on the previous thresholds estimated from the FCME algorithm is applied [11]. One of the most important benefits of the median filter is the reduction of the estimates' variability. It is possible to understand med-FCME through an example: Consider the *i*-th sweep (the total number of sweeps is *M*), med-FCME sorts all the thresholds (from the first threshold to the *i*-th threshold) estimated from FCME in ascending order and after it evaluates the median. The median threshold is new med-FCME threshold for the *i*-th sweep. In particular, in this work the final threshold used for evaluating the spectrum occupancy for the *i*-th sweep is given by

$$\gamma_{\mathrm{i}} = \alpha_{\mathrm{i}} + 3 \text{ [dB]}, \tag{9}$$

where γ_{i} is the final threshold used for the *i*-th sweep and α_{i} is output of med-FCME. ITU-R recommends to use a detection threshold 10 dB above the noise floor [1]. In this work, the detection threshold (γ_{i}) is 3 dB above the noise floor estimate (α_{i}). Hence, this choice allows to improve the sensitivity of the spectrum occupancy analysis and to detect a bigger amount of interference.

3.2.3. Spectrum occupancy computation

The received frequency domain power sample $P_{(i,c)}$ achieved through energy detection is compared to the threshold γ_{i} ($\gamma_{\mathrm{i}} = \gamma$ if the threshold is fixed) obtaining a binary matrix **D**. It is composed by element **D**(*i,c*)

$$D_{(i,c)} = \begin{cases} 1\,, & \text{if } P(i,c) > \gamma_{\mathrm{i}} \\ 0\,, & \text{if } P(i,c) \leq \gamma_{\mathrm{i}} \end{cases}, \tag{10}$$

where $i = 1,2,...,M$ is the sweep index and $c = 1,2,...,N$ is the frequency domain power sample index. [18], [35–37] The binary matrix **D** has a size [*M*]x[*N*].

After the matrix computation, it is easy to evaluate the parameters FCO, FBO and SRO. This work mainly analyzed FCO and FBO. FCO_{c} is found for a frequency value *c* by summing the number of ones in the *c*-th column of matrix **D** and dividing that sum by the total number of sweeps (*M*), i.e.,

$$FCO_{\mathrm{c}} = \frac{\sum_{i=1}^{M} D_{(i,c)}}{M}. \tag{11}$$

Hence, FCO is a vector of size *N* [18]. FBO_{i} is found for a single sweep *i* by summing the ones on the *i*-th row of matrix **D** and dividing that sum by the total number of samples (*N*), i.e.,

$$FBO_{\mathrm{i}} = \frac{\sum_{c=1}^{N} D_{(i,c)}}{N}. \tag{12}$$

FBO_{τ} at an integration time τ is given by

$$FBO_{\tau} = \frac{\sum_{i=1}^{M_{\tau}} FBO_{\mathrm{i}}}{M_{\tau}}, \tag{13}$$

where M_{τ} is the number of sweeps during the integration time τ [18].

3.3. Algorithms analysis

This section describes the algorithms that implement the theoretical concepts studied previously in Section 3.2. The algorithms used in this work perform these tasks:

1. Input data analysis.
2. Threshold evaluation.
3. Spectrum occupancy evaluation analysis.

3.3.1. Input data analysis

The input data depends on:

1. Environment selected.
2. Measurement equipment.
3. Measurement parameters.
4. Duration of monitoring (T_{T}).

These factors are analyzed for each case of study in the following chapters. In every case, the input data is a matrix formed by the power samples that have a size [*M*]x[*N*]. The power samples are given in dBm. *M* mainly depends on the duration of monitoring, *N* mainly depends on the measurement parameters and the amplitude of the power samples depends on all the factors mentioned above. An example of an input data matrix is shown in Figure 12.

3.3.2. Threshold evaluation

In this work, the data is processed with two kinds of thresholds:

1. Fixed threshold.
2. Dynamic threshold.

The fixed threshold has got a value chosen by the system designers according to the principles explained in Section 3.2.2. The dynamic threshold is calculated through the med-FCME algorithm that process the input data matrix (Section 3.3.1) according to the equations (7), (8), (9). At the end, the med-FCME algorithm gives a dynamic threshold for each sweep. The only parameter that the developer chooses is PFA_{DES}. In this work, PFA_{DES} = 5%.

In the first case, the threshold has got a pre-set value, so it doesn't change according to the data, but it allows to use a data post-processing code with a low computational complexity. In the other case, the threshold changes according to the variations of the samples, but the computational complexity is very high.

Sweeps	1	2	3	4	5	6	7	8	9	10	11	12
1	-93.1820	-92.6570	-91.4350	-100.8810	-97.7680	-99.6590	-96.6650	-99.3580	-96.6040	-106.0500	-96.9910	-96.7700
2	-101.3940	-101.4910	-97.2990	-104.5110	-97.6960	-104.5050	-98.6100	-105.5460	-97.5630	-97.1060	-91.6640	-94.8640
3	-94.2330	-93.6820	-93.2230	-93.6370	-102.2460	-107.4320	-94.8900	-101.4530	-94.3550	-99.3240	-95.9700	-106.7880
4	-99.2400	-105.4840	-98.3860	-100.8140	-96.1770	-100.8240	-96.9730	-97.5500	-96.2660	-101.3570	-102.7780	-102.9120
5	-91.4930	-95.2890	-91.0490	-92.7600	-91.5620	-94.3760	-91.4570	-102.4590	-108.6330	-111.5320	-94.4820	-93.3120
6	-91.4930	-95.2890	-91.0490	-92.7600	-91.5620	-94.3760	-91.4570	-102.4590	-108.6330	-111.5320	-94.4820	-93.3120
7	-98.2600	-99.6330	-97.1160	-99.1570	-94.3310	-100.8420	-94.4700	-98.4090	-92.6060	-94.8120	-100.0660	-102.4280
8	-97.9840	-102.2140	-96.4900	-96.8870	-95.0460	-100.7850	-102.9580	-109.6010	-96.9450	-101.5500	-96.5560	-105.7940
9	-91.4810	-99.5180	-92.7190	-94.5650	-92.3950	-100.3770	-97.9420	-108.7560	-103.0300	-111.1260	-101.5500	-101.0790
10	-94.2580	-104.1230	-97.1320	-97.6390	-95.9770	-96.3530	-97.3950	-102.9270	-96.6180	-100.6140	-96.2400	-99.9460
11	-95.3890	-98.2700	-97.4920	-104.3980	-97.4940	-100.0130	-98.4630	-107.0750	-96.2830	-94.4410	-93.5060	-102.3920
12	-96.3720	-92.7420	-92.5750	-105.6920	-93.8810	-99.8210	-94.4800	-107.7460	-99.0330	-99.4950	-94.2730	-98.0340
13	-97.8100	-94.2750	-93.9890	-94.2560	-97.9860	-99.6140	-97.7970	-112.1820	-97.7380	-98.4000	-97.7000	-100.2560
14	-93.6430	-94.9070	-93.3600	-98.6890	-100.3260	-110.2090	-95.2620	-92.1470	-92.4540	-101.3680	-105.7390	-118.5920
15	-95.5890	-98.3360	-96.7590	-106.6370	-97.2330	-99.2770	-94.7870	-97.1310	-90.4380	-92.2060	-89.9970	-98.4200
16	-91.3720	-98.9720	-94.4670	-91.3610	-91.7100	-97.9580	-93.2290	-95.1060	-95.9240	-97.2270	-95.7100	-98.0180
17	-94.2900	-101.8830	-97.6740	-106.5170	-96.1070	-100.0680	-96.1870	-105.9160	-94.7650	-94.5230	-92.7770	-98.9910
18	-96.1470	-96.9780	-94.5130	-101.7360	-98.3830	-101.8910	-96.1260	-93.0700	-93.0060	-95.8800	-98.7270	-103.5250
19	-91.1760	-97.1930	-96.4570	-107.1140	-93.5610	-92.5390	-92.4460	-94.5290	-99.5370	-100.1250	-94.2240	-103.9930
20	-94.8400	-95.7500	-89.4440	-99.0720	-89.7580	-97.1640	-95.7230	-101.6130	-95.4130	-94.9050	-94.8620	-95.6870
21	-99.4560	-104.5970	-98.8500	-106.2290	-98.0210	-104.2980	-97.0380	-96.5470	-91.7130	-92.1530	-91.2680	-108.3230
22	-96.9430	-102.3600	-93.4710	-101.6900	-93.4900	-99.5230	-93.4390	-105.4180	-96.6580	-99.9240	-95.2020	-97.2150
23	-95.0040	-96.6900	-94.4560	-94.2130	-93.4050	-106.3280	-102.9970	-105.3620	-98.8980	-101.5180	-95.7720	-95.3420
24	-89.0680	-90.4620	-94.6580	-98.0250	-90.9650	-92.7130	-98.0490	-98.8030	-98.0090	-101.5630	-99.2610	-99.9830
25	-93.1800	-96.7090	-91.7150	-93.3040	-91.7290	-94.7300	-97.8500	-101.9570	-97.1900	-107.9510	-98.1450	-99.6080
26	-90.7410	-99.4930	-94.2080	-101.4950	-94.2540	-96.9890	-95.6600	-96.1370	-93.2640	-106.8210	-93.4120	-95.7150
27	-94.8540	-105.4310	-101.1790	-103.1780	-97.1890	-99.9560	-96.8660	-100.8810	-97.0990	-98.1260	-97.6440	-107.0990
28	-96.5990	-97.8880	-91.7000	-102.5300	-94.0360	-106.3000	-94.2510	-103.4580	-100.1900	-105.2110	-96.5620	-95.9940
29	-95.1030	-100.3940	-98.2100	-103.6340	-94.0450	-94.7630	-93.7240	-96.7800	-97.4620	-97.7660	-97.3990	-98.2710
30	-97.6410	-103.7940	-93.9950	-95.9330	-94.0060	-95.5860	-92.9470	-100.1990	-95.8690	-95.7000	-95.1140	-105.4020

Frequencies

Figure 12. Input data matrix of size [30]x[12].

The performances of the algorithm based on a fixed threshold and of the algorithm that uses a dynamic threshold are discussed and compared in Chapter 5. In Chapter 5, an algorithm that exploits both the benefits of the algorithm based on a fixed threshold and of med-FCME has been proposed.

3.3.3. Spectrum occupancy evaluation analysis

Whatever is the choice of the threshold, the implemented code process the input data matrix according to the equations shown in Section 3.2.3. At the end, it is achieved a digital matrix **D** according to (10) and through that, it is possible to evaluate FCO using equation (11) and FBO according to the equation (13). The code is able to evaluate also the waterfall and the percentile. These parameters are not directly connected to the problem of spectrum occupancy evaluation, but can give important informations about the distribution of data power in a band.

The **Waterfall** is a 3-D graphic that has time (expressed in second) on x-axis, frequency (expressed in MHz) on y-axis and power (expressed in dBm) on z-axis.

The **Percentile** is a statistical parameter that indicates the value below which a given percentage of observations in a group of observations fall. For example, the 30th percentile is the value below which 30 percent of observations is found [38].

Figure 13 represents the scheme of the implemented code. The input values are in red, the output values are in black and the implemented algorithms are in blue boxes. Figure 13 shows that the fixed threshold is an input value, chosen by the system designers. Otherwise, the dynamic threshold is achieved using the FCME algorithm and a median filter (i.e., med-FCME). The computational complexity necessary to achieve a dynamic threshold is evident.

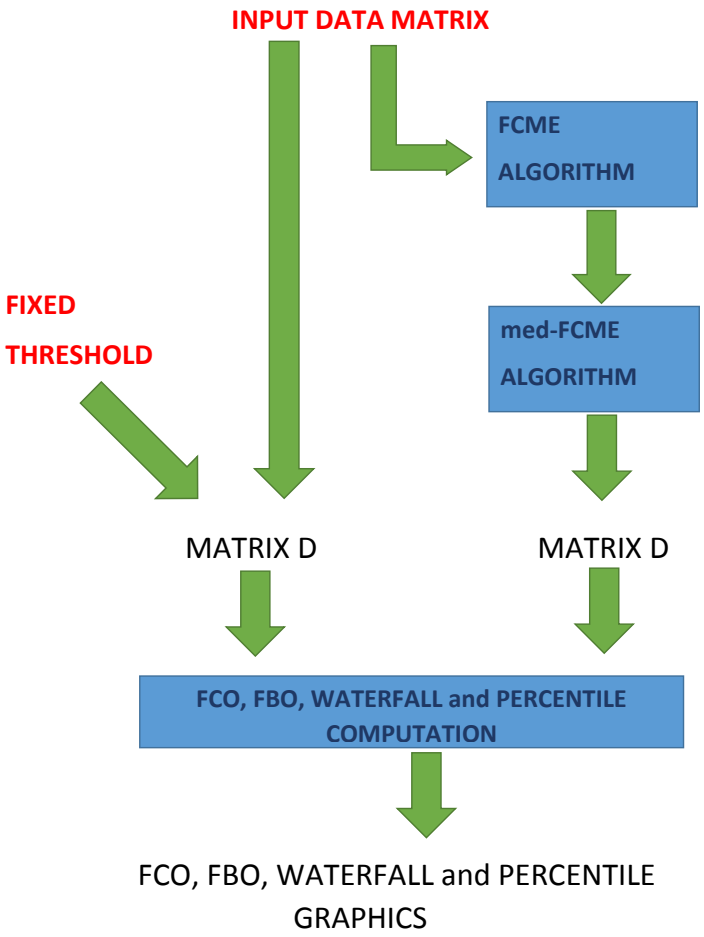

Figure 13. Data analysis process.

4. ENVIRONMENTS AND MEASUREMENT SET UP

This chapter describes the environments in which measurement campaigns were carried out in order to assess the level of occupancy of the ISM band. The chapter is structured as follows. Initially the environments are examined, next the equipment and the measurement parameters characterizing every measurement campaign are studied.

4.1. Environments

In this work, several scenarios that can be identified as potential scenarios for WBAN use are examined. The environments analyzed are:

- Office.
- Home.
- "San Giuseppe" hospital.
- Oulu University Hospital.

4.1.1. Office and Home

The office considered in the measurement campaigns is a modern office, situated in the city of Florence, Italy. It is surrounded by other offices and houses. In this office, there are several internal WiFi (Wireless Fidelity) access points and also the city offers a WiFi free access network for public use, received in the office. The home, situated in Florence, has got similar features of the office, the main difference is the lack of the public WiFi. [39]

4.1.2. "San Giuseppe" hospital

"San Giuseppe" hospital is situated in Empoli, a medium-size town close to Florence, Italy. The hospital is formed by four buildings and has got a surface of 43402 square meters, totally. In the hospital, there are 24 wards, 413 beds, 8 operating rooms and 2 birthing rooms. The recovery beds are equipped with a computer that can exploit the hospital WiFi network. "San Giuseppe" hospital is a modern hospital that utilizes the latest medical devices. These devices use the wireless connection for transmitting medical data to the electronic patient record and for updating the health history of each patient. [30], [39]

Figure 14 shows the map of the emergency ward. The perimeter of the emergency ward is represented by the green solid line. The blue dotted line shows the perimeter of the area where the ambulances accede to bring the patients in the emergency ward. The purple dashed line defines the perimeter of the triage and of the waiting room. [40] The spot where the measurements were carried out is represented by the red point. The interference sources such as the WiFi access points or the hospital devices, are represented by the green, blue and yellow points.

Different zones have different functionalities, in particular:

- In corridor 1, there are several types of ambulatory care units [38].
- Corridor 2 is utilized for bedridden patients that have various health problems from grievous diseases to low-risk health conditions [38].
- Corridor 3 is utilized for radiological analyses: X-ray, tomography, magnetic resonance imaging (MRI), ultrasound, etc. In this corridor there is also a "red room" utilized for red code operations (intensive care and surgery) [38].

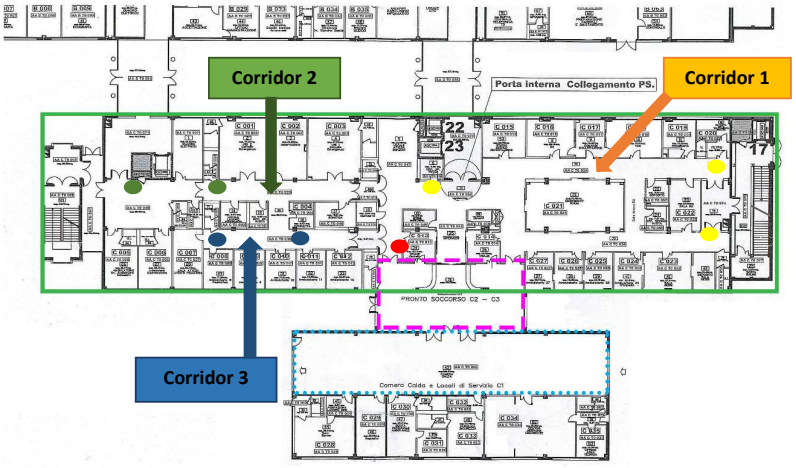

Figure 14. Map of the emergency ward of "San Giuseppe" hospital.

4.1.3. Oulu University Hospital

Oulu University Hospital utilizes the latest equipment in all specialized branches of medicine. The hospital provides a free WiFi network for public use and it is available almost in every wards. The hospital provides 900 beds. Oulu University Hospital is the biggest hospital of the Ostrobothnia, it welcomes the sickest patients from all the parts of this region. The measurements were carried out in the accident and emergency ward, shown in Figure 15 and in the daily surgery ward, shown in Figure 16. The spot where the spectrum analyzer used in the measurements was placed is represented by red triangle.

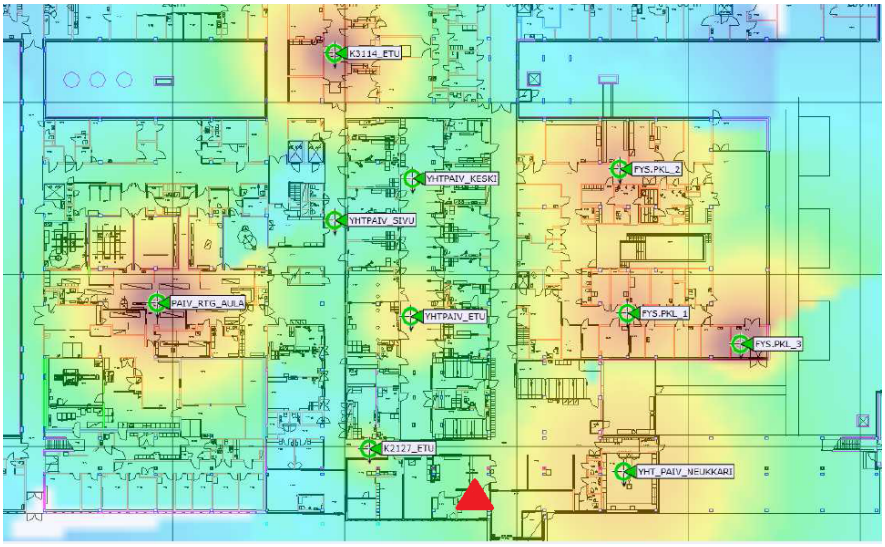

Figure 15. Map of the accident and emergency ward of Oulu University Hospital.

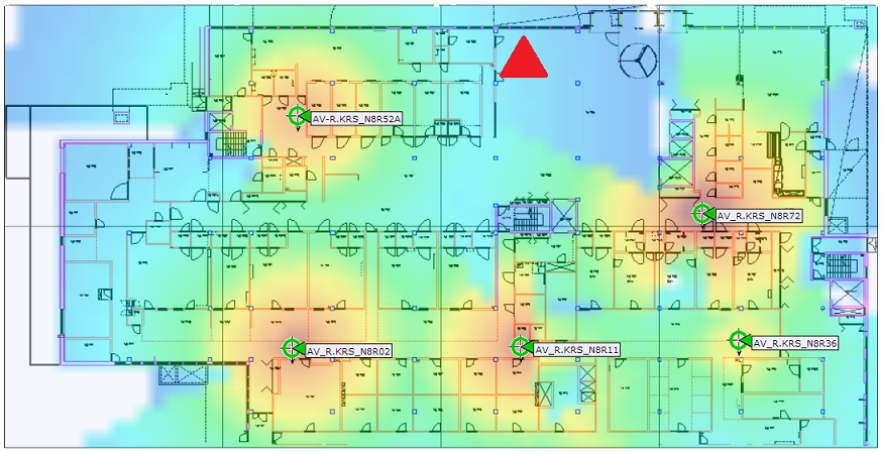

Figure 16. Map of the daily surgery ward of Oulu University Hospital.

4.2. Measurements

In this section the measurement equipment and the measurement parameters used for collecting data in the environments previously introduced are described. The equipment utilized in the measurements is composed by [30]:

1. An antenna, a band pass filter and a spectrum analyzer for the spectrum sensing.
2. A disk drive for the sample collection and storage.
3. A PC to control the SA.

4.2.1. "San Giuseppe" Hospital

The measurements carried out in "San Giuseppe" hospital were made during the busiest time of the day. In these hours, there are many medics and patients moving around in the hospital. The measurement equipment was put in the emergency ward that includes the medical devices which can transmit wireless signals.

The ISM band was considered, precisely the band B_{S} = [2.400, 2.480] GHz. The received power (in dBm) was measured by a Radio Frequency Explorer spectrum analyzer [38]. The SA used in the Italian measurement campaigns is shown in Figure 17 [41]. The main parameters of the SA are shown in Table 3. Data were collected in about 7 days from 5/7/2014 at 17:56 to 12/7/2014 at 20.24. In this week, the SA makes several breaks of few minutes. Hence, the monitoring phases on which the SA works continuously are separated by breaks of few minutes. In this week, the monitoring phases are 9. In this period, about 7850000 sweeps were collected.

Table 3. Key parameters for the measurements carried out in July

Parameter Name	Value
Frequency Range	2400-2480 MHz
Frequency Resolution	1 kHz
Average Noise Level	-115 dBm
Amplitude Resolution	0.5 dBm
Band Observation Time	120 ms
Frequency Bins	112

4.2.2. Office and Home

In the office and in the home environments, the measurements were undertaken using the devices and settings already examined in the previous section. For the office, data was collected in about 9 days from 3/2/2014 at 10.30 to 12/2/2014 at 10.01 (in the following chapters, this data set is called weekly data set, even if data are collected in 9 days). In this period, about 8500000 sweeps were collected, during 5 monitoring phases. At home, data was collected in about 7 days from 18/2/2014 at 21.56 to 25/2/2014 at 6.37. In this period, about 7000000 sweeps were collected, during 6 monitoring phases.

Figure 17. SA utilized in the Italian measurement campaigns.

4.2.3. Oulu University Hospital

Two measurement campaigns were carried out at the Oulu University Hospital, the first one in December 2014, the second one in June 2014. The measurements were carried out using a spectrum analyzer Agilent E4446A linked to a laptop. MATLAB was connected directly to the spectrum analyzer through Instrument Control Toolbox. In this way, it was possible to control the SA and to analyze the measurement results on site. The spectrum analyzer was connected to an omnidirectional, wideband antenna ARA CMA-118/A through a 1 m length cable. The setup used in the December measurements is shown in Figure 18.

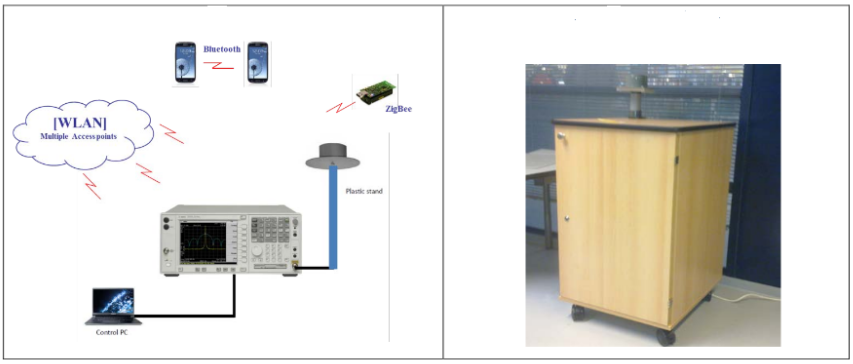

Figure 18. On the left: logical measurement set up, on the right: actual cabinet that contains SA, antenna and control PC.

In June, the measurements were carried out using almost the same setup than December. The main difference is that in June, a low noise amplifier between the SA and the antenna was used to improve the sensitivity of SA.

In December, the measurement equipment was placed near the reception area at the daily surgery building shown in Figure 16. Patients had fixed time to meet a doctor so

they didn't stay there too long. In June, the measurement equipment was placed in the accident and emergency ward (Figure 15), where people come if they don't have or get an appointment with a doctor. Medical conditions are prioritized first and the patients might, in the worst case, need to wait several hours before seeing a doctor. Hence, in this case, the probability that patients exploited the WiFi connection, provided by the Oulu University Hospital, is very high. The key parameters of December's and June's measurement campaigns are listed in Table 4 [18]. In December and June about 24000000 and 14600000 sweeps were collected, respectively.

Table 4. Key parameters for the measurements carried out in December and in June

Parameter Name	December value	June value
Frequency Band	2.35-2.50 GHz	2.35-2.50 GHz
Bandwidth	150 MHz	150 MHz
Frequency Bins	1601	1200
Resolution Bandwidth	300 kHz	240 kHz
Bin-width	93.7 kHz	125 kHz
No. of sweeps	10000	5000
Sweep Time	2 ms approx	3 ms approx
Processing Time	22 ms	45 ms
Band Observation Time	24 ms	48 ms
Integration Time	4 minutes	4 minutes
Measurements Duration	7 days	7 days

5. SPECTRUM OCCUPANCY RESULTS

In this chapter, the results of the spectrum occupancy analyses are discussed. The analyses are carried out using data collected in office, home, "San Giuseppe" hospital and Oulu University Hospital environments. In every analysis waterfall, percentile, FCO and FBO are computed.

This chapter presents a section for every parameter mentioned above. In every section, the informations that the parameter provides and the limits of the parameter used are analyzed.

Finally, Section 5.5 presents a discussion about the results achieved in the analysis and it suggests the implementation of a new post-processing code that exploits both the advantages of algorithms based on the fixed threshold and of algorithms based on the dynamic thresholds.

5.1. Waterfall

Waterfall shows graphically how the interference powers in time and frequency domains are distributed. Waterfall graphics for each environment analyzed are computed, considering, in every case, data collected during a week.

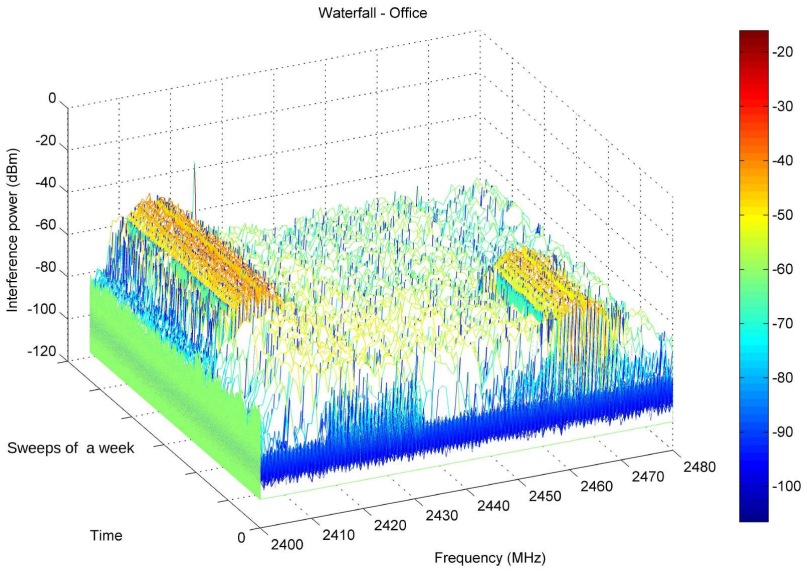

Figure 19. Office, one week measurements.

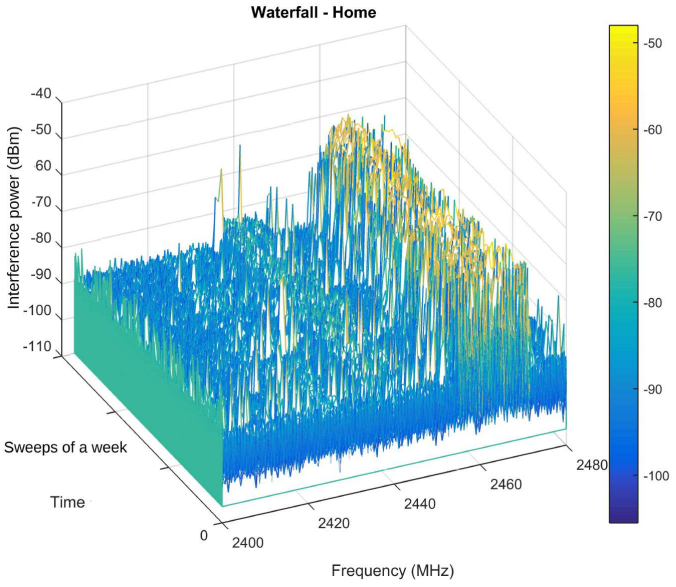

Figure 20. Home, one week measurements.

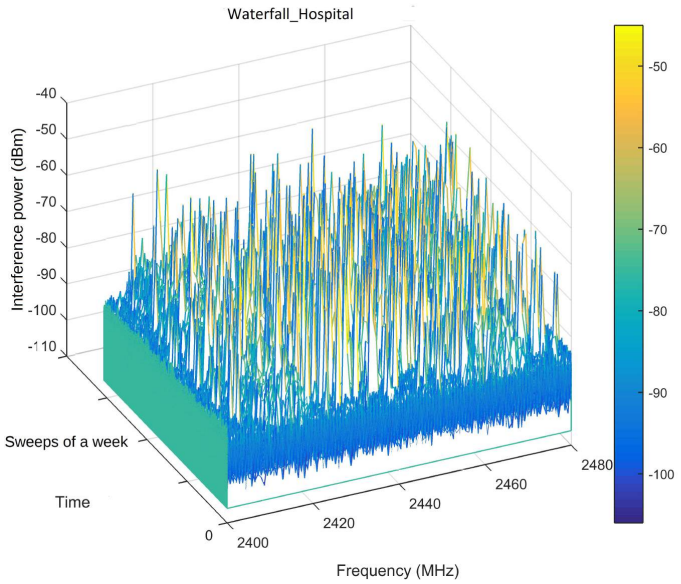

Figure 21. "San Giuseppe" hospital, one week measurements.

The waterfalls represented in Figure 19 and 20 show clearly the frequencies and the sweeps that provide the highest values of interference power. In the office environment (Figure 19), the interference power is remarkable in the frequency range 2400-2430 MHz (WLAN channel 1) in the last days of the week and in the frequency range 2455-2475 MHz (WLAN channel 11) in the first days of the week.

In the home environment (Figure 20), the waterfall presents high interference power in the frequency range 2455-2475 MHz (WLAN channel 11) in all the sweeps of the week. Reason is that there is only one AP, which uses WLAN channel 11.

The waterfall in Figure 21 doesn't highlight interference power. The other graphics, related to "San Giuseppe" hospital, Figures 26, 33, 36, highlight the presence of interference power in this environment. Waterfall doesn't allow visually to distinguish the interference from the noise. Hence, in this case, the waterfall provides graphical informations that are not understandable by human eyes.

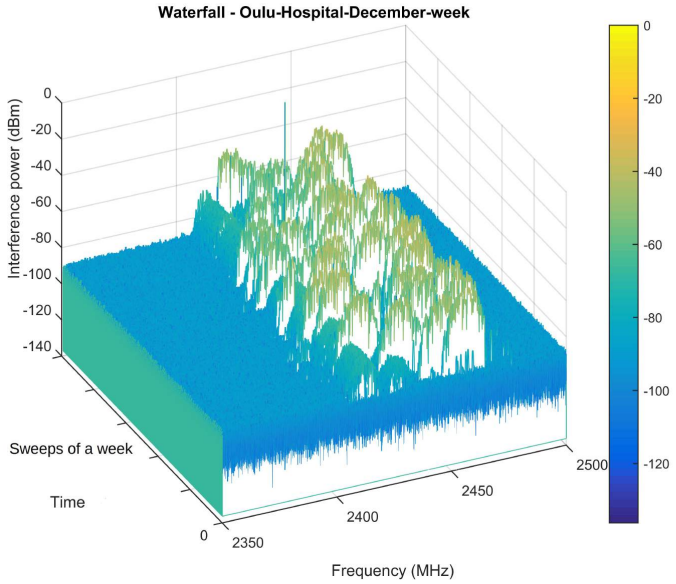

Figure 22. Oulu University Hospital, December, week measurements.

The waterfalls in Figure 22 and 23 highlight the presence of interference power in the frequency range 2410-2475 MHz, but they don't indicate precisely which are the frequencies that present the highest value of interference. They only indicate a wide occupied frequency range.

Hence, in general, the waterfall provide coarse informations that can't be used for understanding if in a particular channel is present interference signal or not. Hence, other parameters, more accurate, are used.

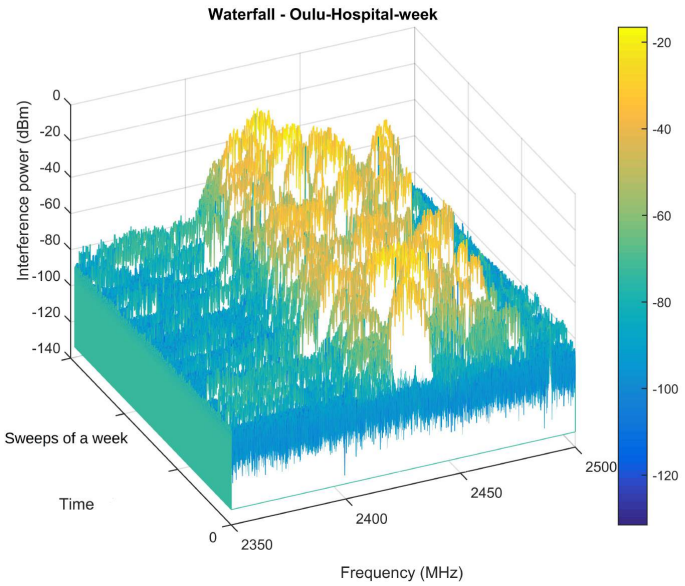

Figure 23. Oulu University Hospital, June, week measurements.

5.2. Percentile

The percentile indicates, for each frequency, the power level below which there is a given percentage of samples. Hence, the p-th percentile graphic defines, for each frequency, the maximum power value below which there are at least the $p\%$ of the samples. Percentile is useful for understanding statistically how the interference samples' amplitude for each frequency is distributed. Percentile graphics for each environment are evaluated, considering, in every case, data collected during a week.

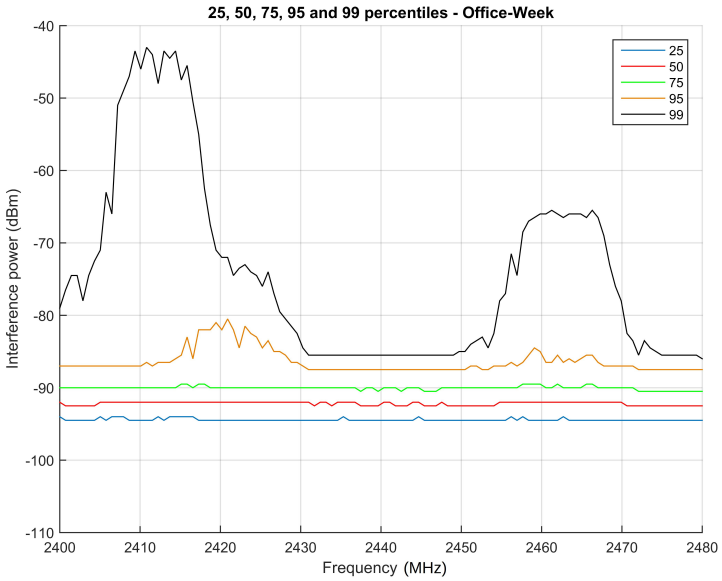

Figure 24. Office, one week measurements. Percentiles 25, 50, 75, 95 and 99.

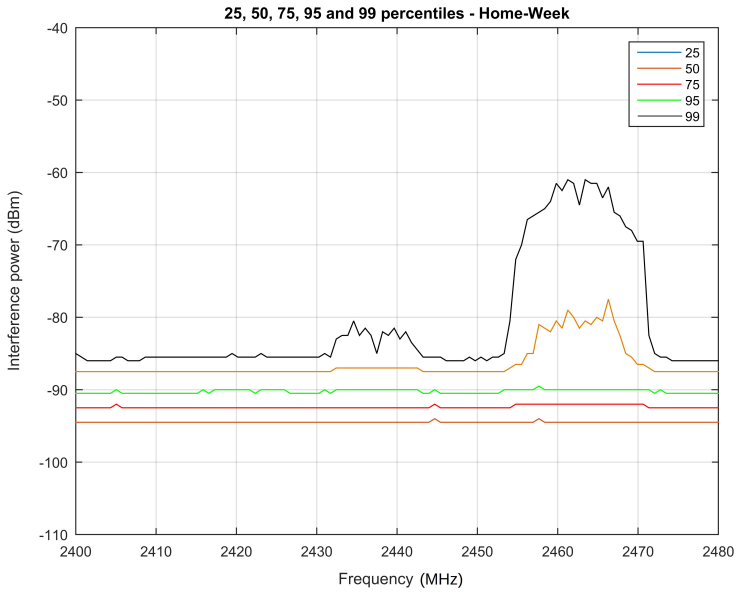

Figure 25. Home, one week measurements. Percentiles 25, 50, 75, 95 and 99.

The percentile represented in Figure 24 confirms that, in office environment, WLAN channels 1 and 11 are used. Figure 25 confirms that, in the home environment, the highest contribution of power is present in WLAN channel 11.

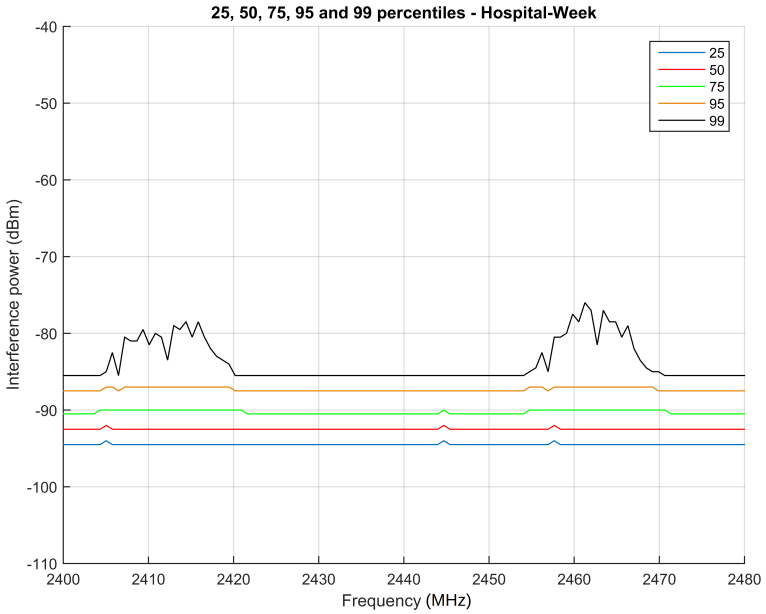

Figure 26. "San Giuseppe" hospital, one week measurements. Percentiles 25, 50, 75, 95 and 99.

The percentile achieved using "San Giuseppe" hospital data, Figure 26, shows that the interference power is low in all the band considered, but in the frequency channels 2405-2420 MHz (WLAN channel 1) and 2455-2470 MHz (WLAN channel 11) the interference power assumes slightly higher values. Hence, in this case, despite waterfall (Figure 21), the percentile highlights the presence of interference power, even if this is very low. In this case, there is a wall between the SA and the AP closest to the SA (the emergency ward of "San Giuseppe" hospital is shown in Figure 14). In this wall, there is a fire door formed also by steel. The door can be opened only pressing a button, hence the door is closed in most of the time. Most of the signals transmitted by the AP are blocked by the door and only a little amount of signals reaches the SA. Hence, the occupancy is low.

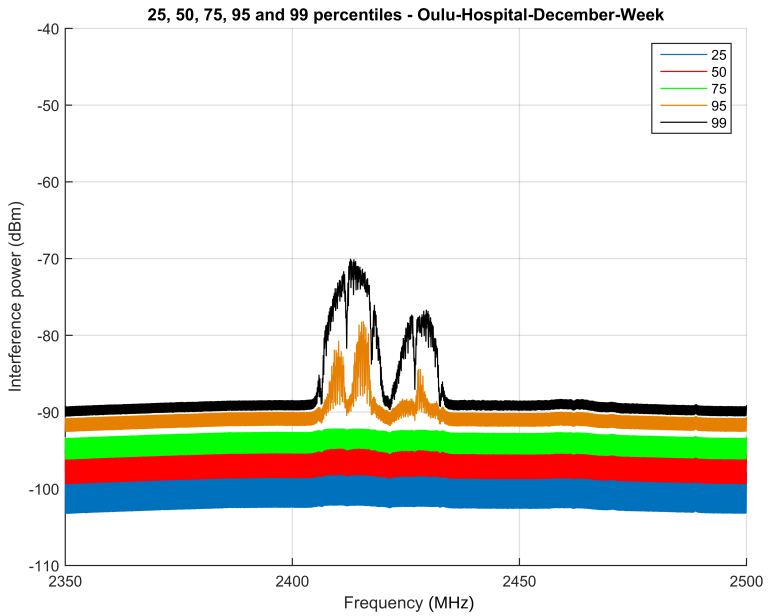

Figure 27. Oulu University Hospital, December, week measurements. Percentiles 25, 50, 75, 95 and 99.

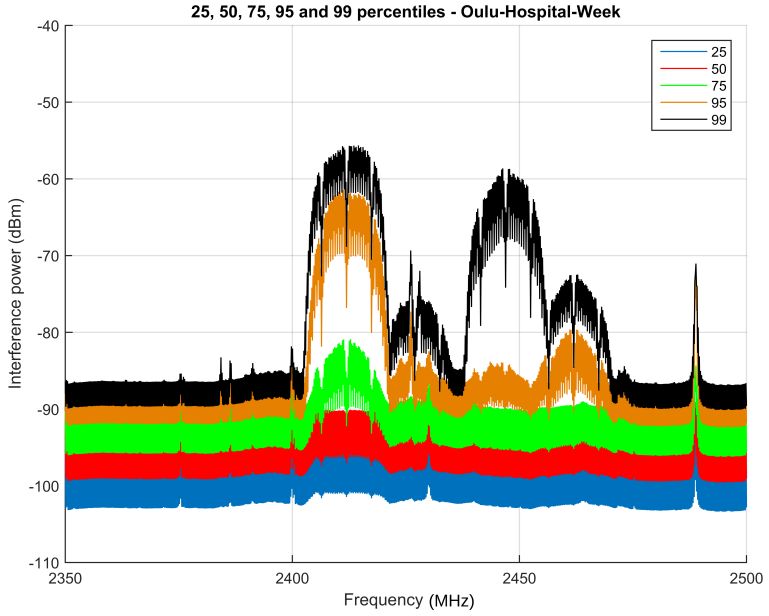

Figure 28. Oulu University Hospital, June, week measurements. Percentiles 25, 50, 75, 95 and 99.

The percentiles achieved using December data of Oulu University Hospital, Figure 27, shows that there are two relevant contributions of interference power in the frequency range 2410-2440 MHz (WLAN channel 1 and 6).

Figure 28 presents five interference power contributions. The figure shows four wideband signals, located in the range 2410-2470 MHz (including WLAN channels 1, 6 and 11), and a narrowband signal at 2485 MHz.

Hence, in general, the percentile gives informations about the frequencial localisations of the interference signal more detailed than the waterfall, but, obviously, it doesn't provide informations about the percentage of occupancy of one channel. So, for making an exaustive spectrum occupancy evaluation, it is necessary to compute other parameters, such as the FCO and the FBO.

5.3. Frequency channel occupancy

FCO defines the occupancy percentage of a particular frequency channel. FCO allows to understand if a frequency channel offers already resources usable for the implementation of a new network, or if the frequency channel is fully exploited by other networks. Frequency channel occupancy is defined in Chapter 3.

In this work, FCOs through a fixed threshold and dynamic thresholds are evaluated. FCO-fixed indicates the FCO evaluated using algorithms based on a fixed threshold and FCO-FCME indicates the FCO evaluated exploiting algorithms based on dynamic thresholds.

The fixed threshold value depends on real measurements carried out in "San Giuseppe" hospital [42], [43]. In those works, a wireless electrocardiogram (ECG) signal, operating in the ISM band, was transmitted for modeling the path loss in the hospital environment. The results highlight that a received power sample below -80 dBm can't provide useful information. In this case, the sample is compromised. -80 dBm can be considered a value that properly separates signals from noise. Hence, the fixed threshold assumes this value [40]. The fixed threshold of value -80 dBm was used also in the home, office and Oulu University Hospital data analysis.

FCOs for each environment are computed. Two interval times in this analysis are considered: one day and one week. Subsequently, FCO-fixed and FCO-FCME, computed using the office data set, are compared. This data was collected during a day (813690 sweeps). The goal is to analyze these graphics to understand the differences between FCO-fixed and FCO-FCME.

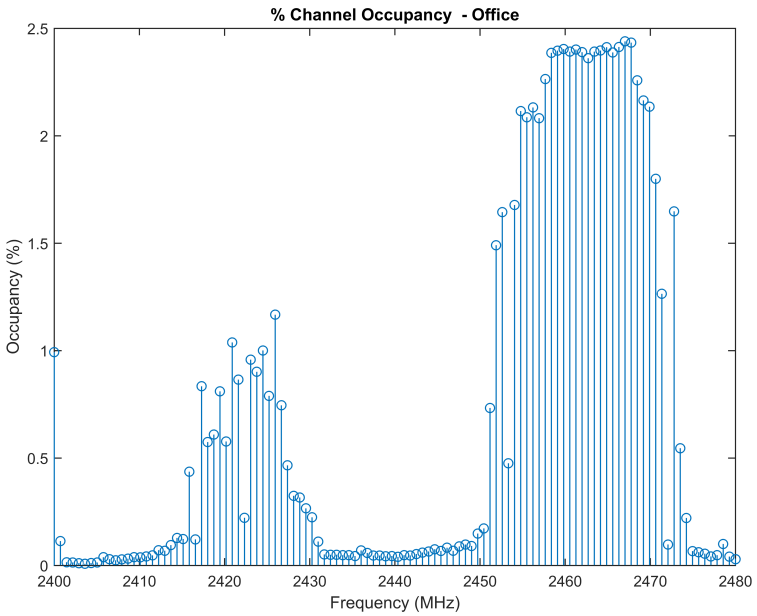

Figure 29. Office, one day measurements. FCO-fixed, threshold equal to -80 dBm.

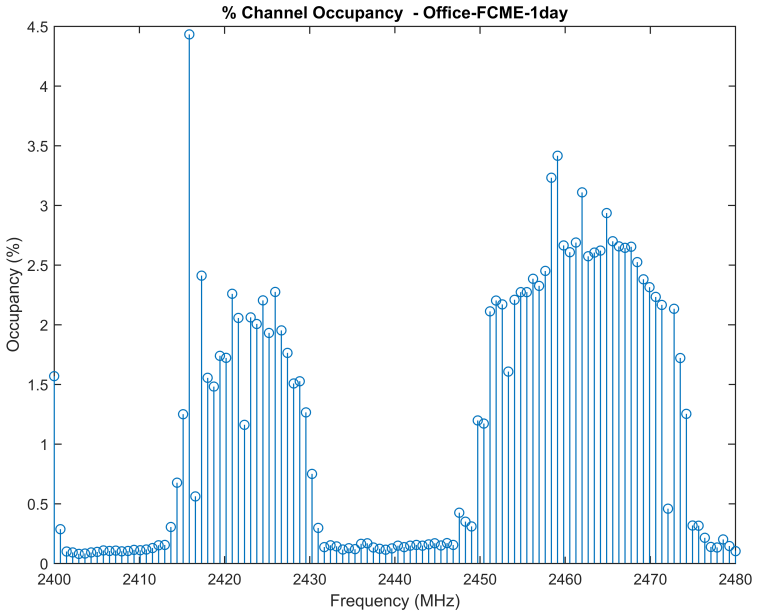

Figure 30. Office, one day measurements. FCO-FCME.

Figures 29 and 30 present differences between the analysis methods, even this difference is only few percentages in decimal values. In other analysis, this difference is more evident. The mean of the dynamic thresholds is -83.6 dBm. It means that the dynamic thresholds are lower than the fixed threshold (-80 dBm). Hence, FCO-FCME is higher than FCO-fixed.

The dynamic thresholds directly depend on the amplitude of data, hence FCO-FCME is more accurate and precise than the FCO-fixed. However, the computational complexity of the algorithm for the evaluation of the dynamic thresholds is considerable and the computing time is very high, mostly if a large amount of data is considered. For example, using data collected in Oulu University Hospital during the measurement campaign in December, the time necessary for computing FCO-FCME and FCO-fixed is four hours and one hour and half, respectively. Despite this, subsequently only the FCO-FCME are reported, because they are considered the best results for analyzing the channel occupancy. The graphics reported below are carried out using the data collected during a whole week.

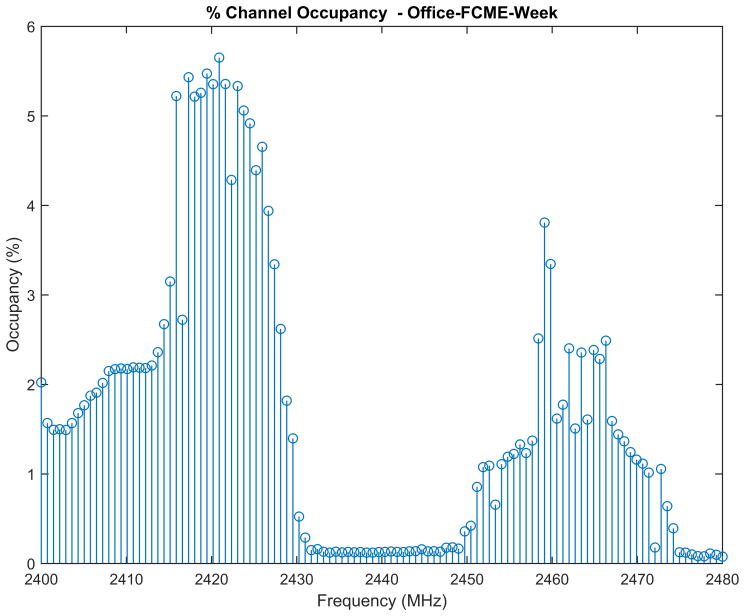

Figure 31. Office, one week measurements. FCO-FCME.

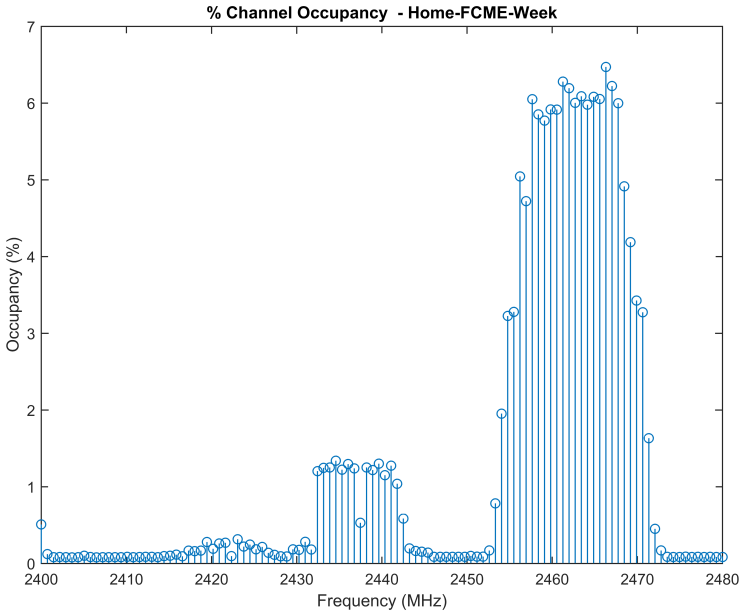

Figure 32. Home, one week measurements. FCO-FCME.

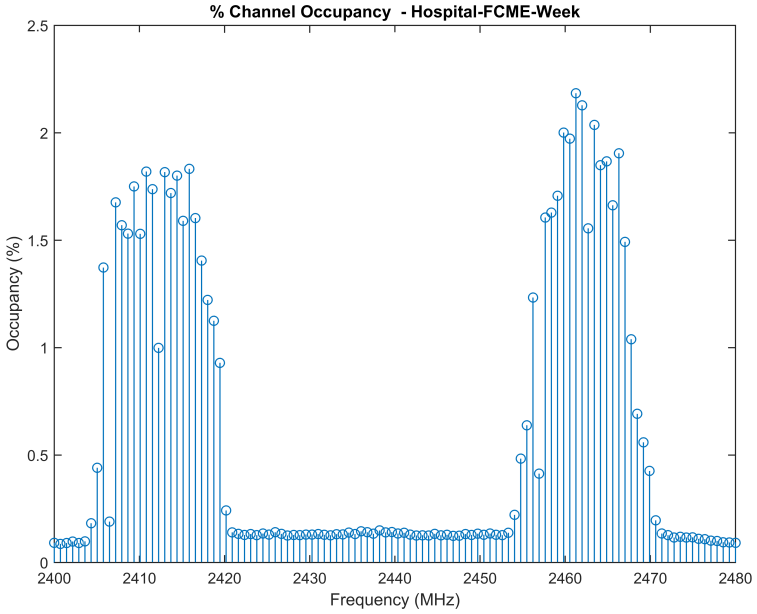

Figure 33. "San Giuseppe" hospital, one week measurements. FCO-FCME.

For each environment, the interference power is located in the frequency range already indicated in Section 5.1 and 5.2. Figures 31-34 show low occupancy values. The occupancy values are in the range 0.2-6.5%.

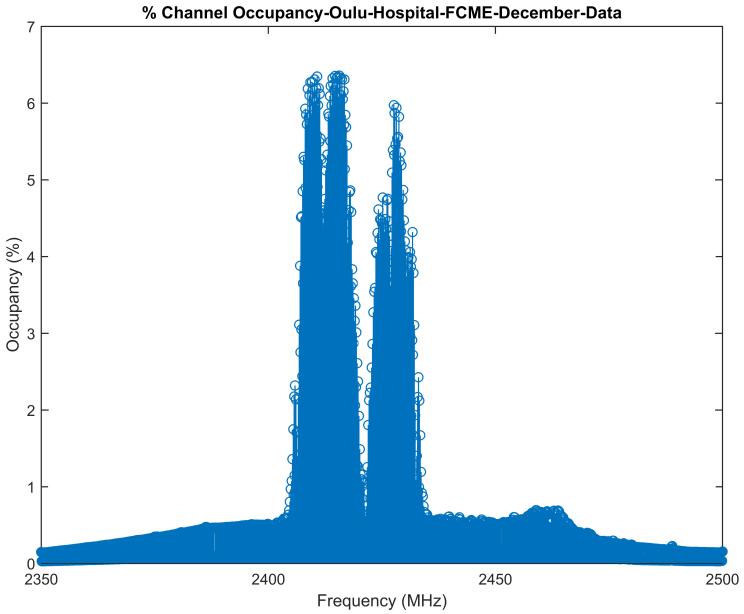

Figure 34. Oulu University Hospital, December, week measurements. FCO-FCME.

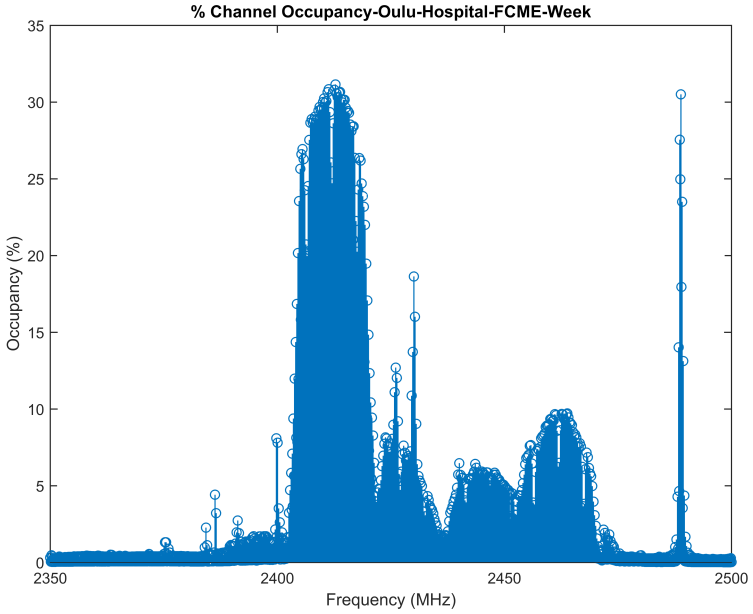

Figure 35. Oulu University Hospital, June, week measurements. FCO-FCME.

The frequency samples considered in the Italian measurement campaigns are 112. The frequency samples considered in the Finnish measurement campaigns are 1601 in December and 1200 in June. Hence, the Finnish FCOs are evaluated considering a number of points greater than the number of points used by the Italian FCOs. This is the reason of the difference between the Italian FCOs (Figures 31, 32 and 33) and the Finnish FCOs (Figures 34 and 35).

The results shown in Figure 35 highlight occupancy values very high, values of 30% are even reached. Considering Oulu University Hospital environment, the difference between the results achieved using December data set and the results achieved using June data set, is evident. This difference depends mostly on the location of the spectrum analyzer. In fact, during December measurement campaign, the spectrum analyzer was placed in the reception area, at daily surgery building (Figure 16). During June measurement campaign, the measurement equipment was located in the accident and emergency ward (Figure 15). In the reception area, at daily surgery building, the patients have a fixed appointment time with the doctor, hence they don't be there too long. In the accident and emergency ward, patients might need to wait several hours, hence the probability that they use an internet connection, through their mobile devices, is very high.

5.4. Frequency band occupancy

FBO defines the frequency band occupancy percentage in the time domain. In this work, FBO is computed using the dynamic thresholds. Frequency band occupancy is defined in Chapter 3. FBOs in the hospital environments are evaluated, considering in every case all data collected during a week.

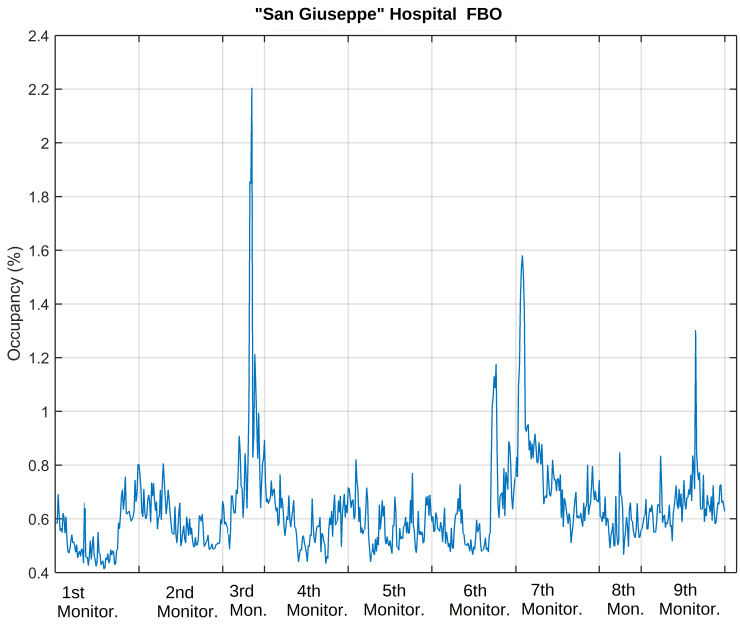

Figure 36. "San Giuseppe" hospital, one week measurements.

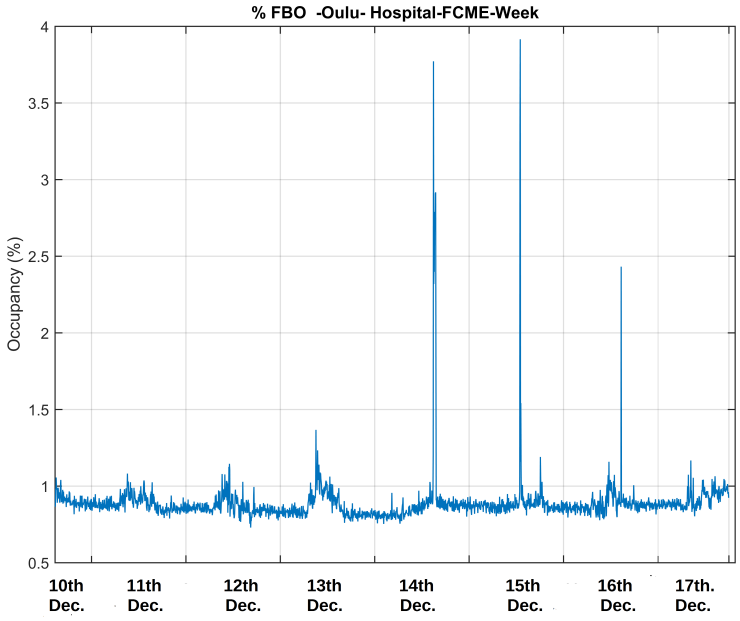

Figure 37. Oulu University Hospital, December, week measurements.

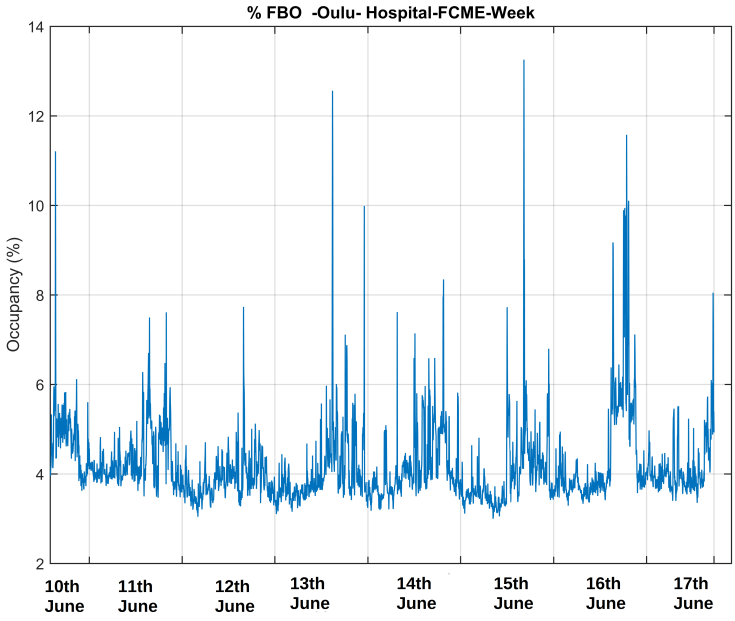

Figure 38. Oulu University Hospital, June, week measurements.

The graphics shown in Figure 36 and 37 present FBO values lower than the FBO values in Figure 38. Hence, also in time domain, data collected in the accident and emergency ward of Oulu University Hospital presents higher occupancy values than data collected in "San Giuseppe" hospital and data collected in the daily surgery building of the Oulu University Hospital.

5.5. Results discussion

The dynamic thresholds, evaluated using med-FCME algorithm, change in a function of the environments and in a function of the amplitude of each sample. In Table 5, the mean of the dynamic thresholds are reported, as a function of the environments analyzed.

Table 5. Mean of the dynamic thresholds, as a function of the environments considered

Mean of the dynamic thresholds	Environment
-83.6 dBm	Office
-83.7 dBm	Home
-83.7 dBm	"San Giuseppe" hospital
-87.9 dBm	Oulu University Hospital, December data set
-84,9 dBm	Oulu University Hospital, June data set

The mean values of the dynamic thresholds achieved using the data collected in the office, home and "San Giuseppe" hospital environments, assume similar values. They cluster around -83.6 dBm. The mean values of the dynamic threshold evaluated considering Oulu University Hospital data set assume lower values: -87.9 dBm, using December data set and -84.9 dBm using June data set.

The difference between thresholds achieved using Italian data set and Finnish data set mainly depends on the band considered. In fact, in office, home and "San Giuseppe" hospital cases, the frequency range observed is 2400-2480 MHz. In both Oulu University Hospital measurement campaigns, the band examined is 2350-2500 MHz. Hence, the post-processing phase carried out in Oulu considers, for calculating the initial dynamic thresholds, samples related to a part of the band (2350-2400 MHz) which is not used. These samples represent the noise floor. The samples amplitude shapes the threshold, hence lower samples mean lower threshold. The post-processing carried out using Florence data, computes the initial dynamic thresholds using samples that belong to a part of the ISM band which is more utilized. This explains the higher threshold values. Hence, the interference present in the Italian environments would be higher than the interference detected, if also the samples in the range of frequencies 2350-2400 MHz were considered for computing the threshold. In fact, considering these samples the threshold would be lower and the occupancy higher.

The following graphic shows the FCO evaluated using the office data set (collected in a week) and a fixed threshold value equal to the related mean of the dynamic thresholds (-83.6 dBm).

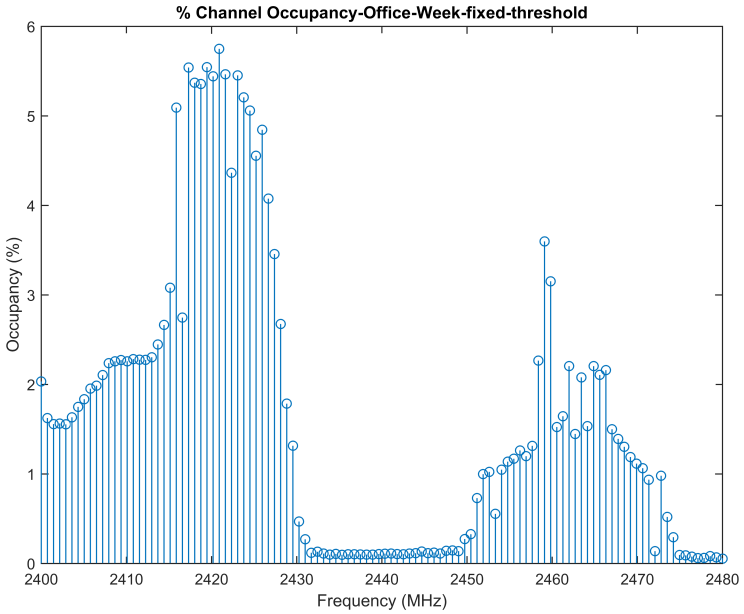

Figure 39. Office, one week measurements. FCO-fixed, threshold equal to -83.6 dBm.

The FCO-fixed shown in Figure 39, having a threshold equal to -83.6 dBm, is equal to the FCO-FCME, computed using the same data (Figure 31). This result is confirmed also by the FCO-fixed, evaluated using data set of the other environments and a fixed threshold equal to the related mean value of the dynamic thresholds (the dynamic thresholds mean values are shown in Tab. 5).

The med-FCME algorithm computes a threshold for every sweep, hence, in every analysis carried out, the number of thresholds is very high. In the following graphics, the dynamic thresholds trends achieved using the data collected in office, home and Oulu University Hospital environments, are reported. These graphics report only an exiguous number of thresholds. The number of thresholds shown in the graphics, as a function of the environment and the time necessary to collect the corresponding sweeps, is represented in Table 6.

Table 6. Number of thresholds as a function of the environment and time to collect the corresponding sweeps

Thresholds number (N_λ)	Environment	Time used to collect N_λ sweeps
5000	Office	10 min.
10000	Home	20 min.
10000	Oulu hospital, December data	4 min.
5000	Oulu hospital, June data	4 min.

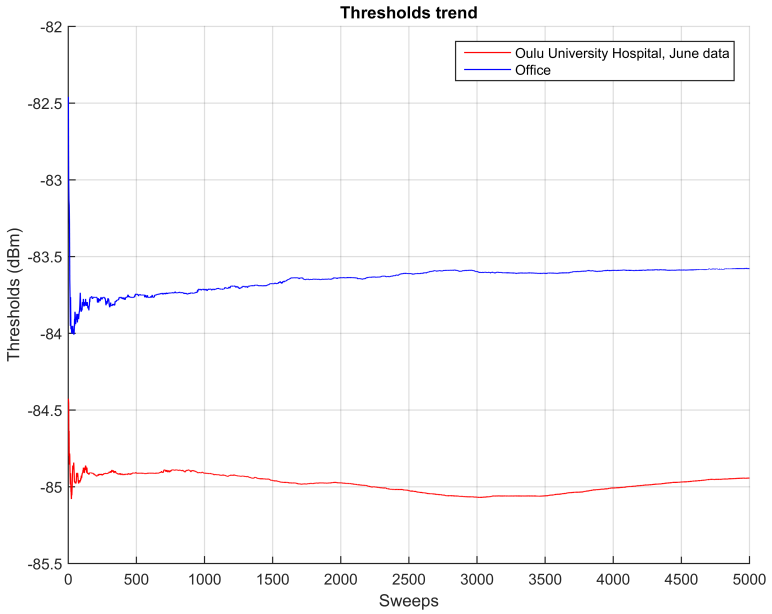

Figure 40. Office and Oulu University Hospital, June data set. 5000 dynamic thresholds trends in blue and red, respectively.

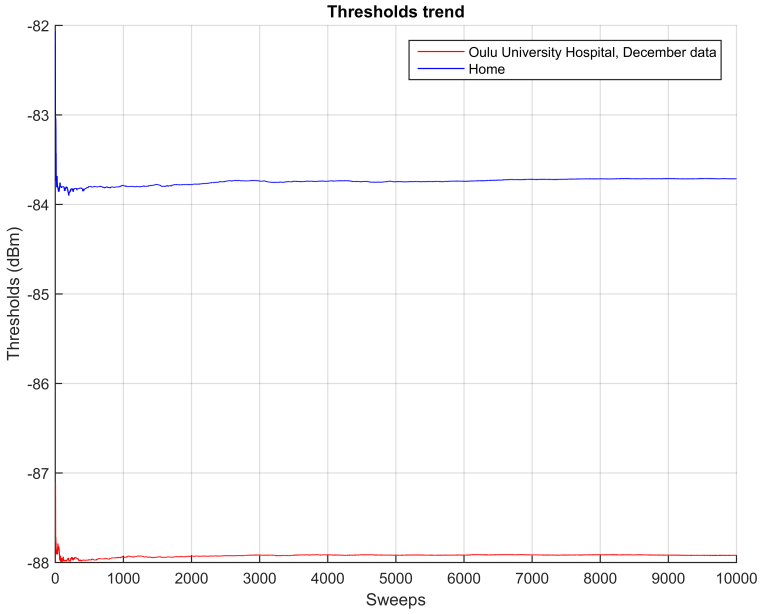

Figure 41. Home and Oulu University Hospital, December data set. 1000 dynamic thresholds trends in blue and red, respectively.

Figures 40 and 41 show that the thresholds' trend, in office, home and Oulu University Hospital (December data set), initially, is oscillatory but, subsequently, the trend is almost flat and it converges to a precise value. Threshold trend related to Oulu Uni-

versity Hospital (June data set) is very oscillatory and it converges only after a large number of sweeps. In every cases, the convergence value is the mean value of the dynamic thresholds. This explains why FCO-FCME is equal to FCO-fixed, evaluated with a threshold equal to the mean value of the dynamic threshold.

Hence, it is not necessary to compute a threshold for each sweep, but it is possible to use a data post-processing code that initially computes the med-FCME thresholds for the first sweeps, then evaluates the thresholds mean value and next assigns this value to the thresholds of the remaining sweeps. The convergence occurs after few sweeps, only in Oulu University Hospital, in June measurement campaign, Figure 40, the trend of the threshold is more oscillatory.

In this way it could be created a data post-processing code that exploits the speed of the algorithms based on the fixed threshold and the effectiveness and accuracy of the algorithms based on the dynamic thresholds.

6. TIME DOMAIN ANALYSIS AND INTERFERENCE MODELLING

In this chapter, the results of the time domain analysis of interference are reported and a mathematical interference modelling, achieved using these results, is described. The analyses are carried out considering the samples in time domain, fixing the frequency. The frequencies considered are the central frequencies of WLAN channel 1 and WLAN channel 6: 2412 MHz and 2437 MHz, respectively. WLAN channel 1 and WLAN channel 6 are examined because, in several environments analyzed, these channels are important interference sources. In fact, WLAN channel 1 and WLAN channel 6 present high values of occupancy in the ISM band.

The time domain analysis allows to examine the features of the clusters. The cluster is a set of consecutive samples of interference, in time domain, that assume a value greater than a threshold.

To investigate carefully the aggregate interference in the ISM band, it is extremely important to know the number of interference samples that form a cluster (i.e., cluster size), the average amplitude of these samples (i.e., cluster amplitude) and the time interval between two consecutive clusters (i.e., interarrival time).

The cluster size, interarrival time and cluster amplitude computation allows to obtain a mathematical interference modelling that can be used to predict the interference trend.

This chapter is organized as follows: Section 6.1 describes the informations provided by the cluster size, the cluster amplitude and the interarrival time parameters. Section 6.2 extracts a mathematical interference modelling using the informations achieved in the previous section.

6.1. Time domain analysis results

In this work, the cluster size, the cluster amplitude and the interarrival time have been derived by using a post-processing code. The post-processing code evaluates the parameters mentioned above, using data collected in the environments described in Chapter 4. The post-processing code returns the cluster size, the cluster amplitude and the interarrival time vectors. In particular, the l-th element of every vector, respectively represents the size, the amplitude and the interarrival time of the l-th cluster. The post-processing code represents these vectors through the related histograms.

The time domain analysis carried out using the post-processing code previously described considers weekly data collected in Oulu University Hospital in December's and June's measurement campaigns. "San Giuseppe" hospital, home and office data are not considered. Data collected in the Italian measurement campaigns can't be utilized due to the measurement equipment used. In fact, in the Italian measurement campaigns, the SA presents a band observation time equal to 120 ms (the key parameters for the Italian measurement campaigns are shown in Table 3). It means that the time interval between two consecutive samples, related to the same frequency, is 120 ms. The interference is characterized by short range communications which occur in time interval shorter than 120 ms. Hence, the SA used in Italy presents an high probability to miss significant interference samples, because the sampling frequency of the SA is smaller

than the frequency of the interference communications. In the Finnish measurement campaigns, the time interval that divides two consecutive samples related to the same frequency is 24 ms in December measurement campaign and 48 ms in June measurement campaign (the key parameters for the Finnish measurement campaigns are shown in Table 4). The band observation times considered in the Finnish measurement campaigns are small, hence, in this case, the probability to miss significant interference samples is low.

The threshold setting assumes a fundamental role for the cluster detection. The post-processing code, implemented in this work, uses a fixed threshold. The value of the threshold is equal to the mean value of the dynamic thresholds, rounded down. In Table 5, the mean of the dynamic thresholds are reported as a function of the environments analyzed.

6.1.1. Cluster size histogram

In this paragraph, the cluster size histograms are reported. The histograms allow to know how many times a particular cluster size is occurred. Only the histograms achieved using WLAN channel 1 samples, related to June data set and WLAN channel 6 samples related to December data set, are reported.

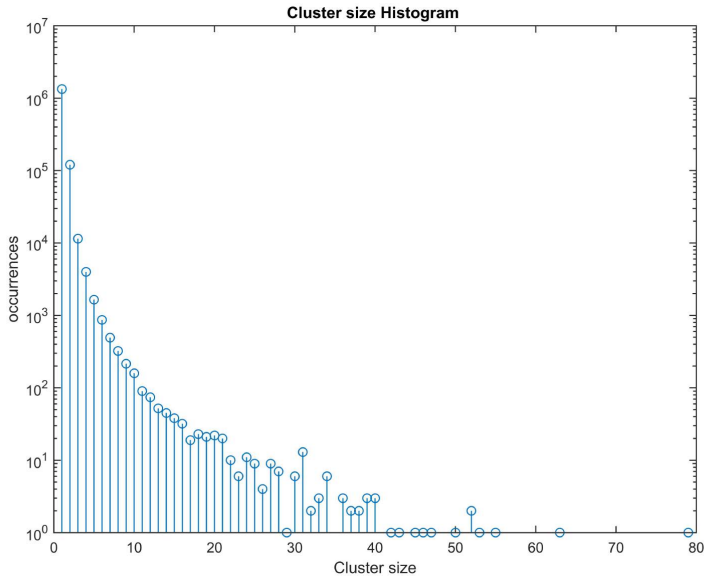

Figure 42. Oulu University Hospital, June, week measurements. WLAN Channel 1.

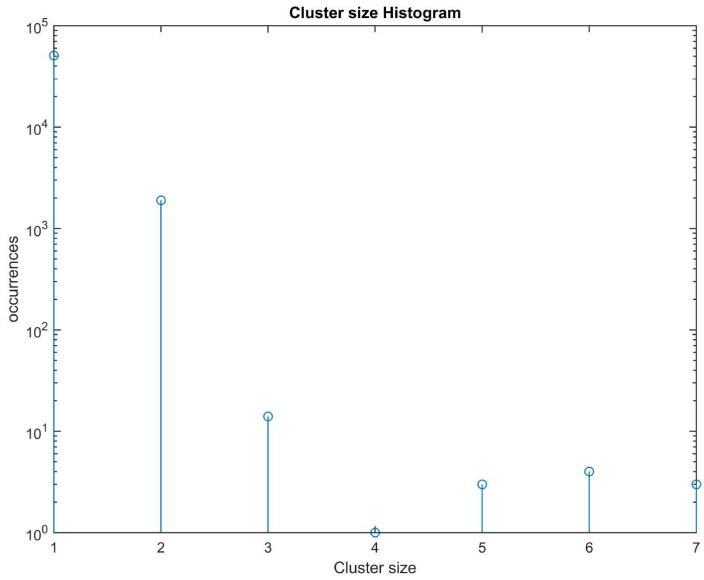

Figure 43. Oulu University Hospital, December, week measurements. WLAN Channel 6.

In the first analysis, Figure 42, the elements of the cluster size vector assume the highest values. There are also clusters which size is 80. This is the "worst" case, because, how shown also in the interarrival time histogram (Figure 44) and in the cluster amplitude histogram (Figure 48), the interference signals, in WLAN channel 1 (June data set), are very strong and the transmission is continuous. In the second analysis, Figure 43, the elements of the cluster size vector assume the lowest values (the maximum size is 7). This is the "best" case, because, how shown also in the cluster amplitude histogram (Figure 47), the interference signals, in WLAN channel 6 (December data set), are weak and the transmission is intermittent. Both the graphics (Figures 42 and 43) show that most of the clusters have a size equal to 1.

6.1.2. Interarrival time histogram

In this paragraph, the interarrival time histograms are discussed. The interarrival time considered is discrete. The discrete interarrival time ($T_{\mathrm{I,D}}$) is calculated as

$$T_{\mathrm{I,D}} = \frac{T_{\mathrm{I,C}}}{T_{\mathrm{Bobs}}} = \frac{z \cdot T_{\mathrm{Bobs}}}{T_{\mathrm{Bobs}}} = z, \tag{14}$$

where $T_{\mathrm{I,C}}$ is the continuous interarrival time and z is the number of samples below the threshold that divide two consecutive clusters.

In this paragraph, the interarrival time histograms related to the data collected in June measurement campaign and achieved considering WLAN channel 1 and WLAN channel 6 samples are represented.

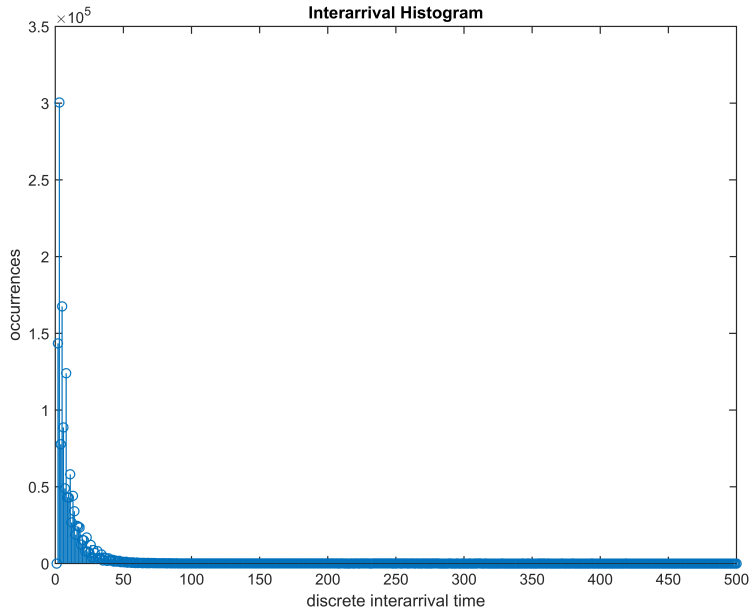

Figure 44. Oulu University Hospital, June, week measurements. WLAN Channel 1.

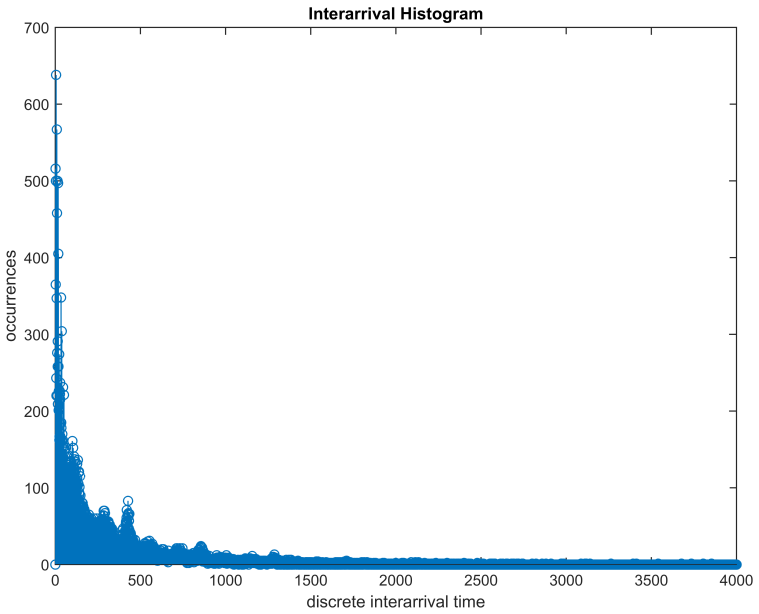

Figure 45. Oulu University Hospital, June, week measurements. WLAN Channel 6.

Figure 44 shows that the elements of the discrete interarrival time vector assume low values. It means that, mostly, the clusters are close to each other. It can be inferred that WLAN channel 1 (related to June data set) is characterized by a transmission that is almost continuous. Figure 44 confirms that WLAN channel 1, related to June data set can be considered as the "worst" case. In Figure 45, the discrete interarrival vector

presents greater values than the previous case. There are also values equal to 4000. Hence, WLAN channel 6 (related to June data set) is characterized by an intermittent transmission. The reason of the big difference between Figure 44 and Figure 45 is the position of the SA. The SA was placed close to an AP that exploits WLAN channel 1. The same difference is present in time domain analysis carried out using December data set. Also in this case, the discrete interarrival time histogram, achieved using WLAN channel 1 samples, suggests that the interference transmission is continuous. Otherwise, the analysis carried out considering WLAN channel 6 samples indicates that the WLAN channel 6 transmission is intermittent (interarrival time equal to 2000, are reached).

6.1.3. Cluster amplitude histogram

In this paragraph, the cluster amplitude histogram graphics are reported. The amplitude represented in the graphics is the average amplitude of the amplitudes of the samples that form a cluster.

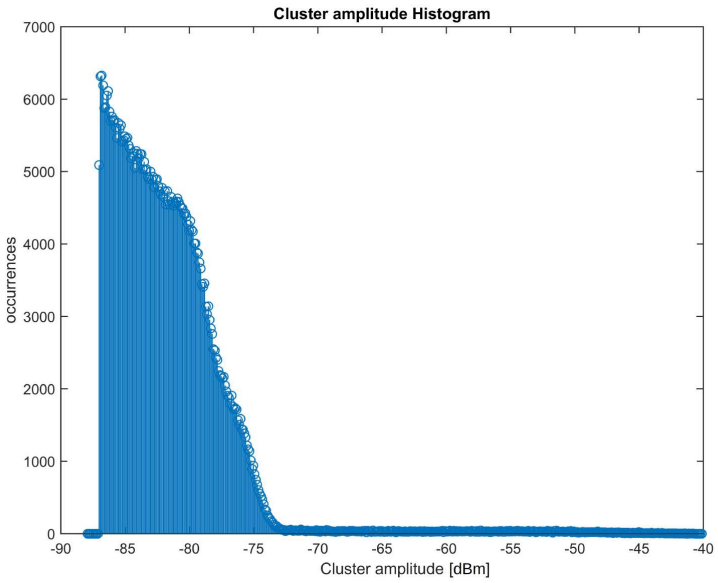

Figure 46. Oulu University Hospital, December, week measurements. WLAN Channel 1.

The clusters' amplitude histograms reported in Figure 46 and 47 are evaluated using December data set. Figure 46 is achieved using samples from WLAN channel 1. Figure 47 is computed using WLAN channel 6 samples. In Figure 46, the cluster average amplitudes are in the range -87÷-73 dBm (-87 dBm is the threshold). In Figure 47, the largest number of clusters' average amplitudes is in the range -87÷-85 dBm. The difference between occurrences shown in Figure 46 and Figure 47 is determined by the distance between AP and SA. The SA was placed close to an AP that exploits WLAN channel 1, hence the WLAN channel 1 samples' amplitudes are higher than WLAN channel 6 samples' amplitudes. Figure 47 confirms that WLAN channel 6, related to

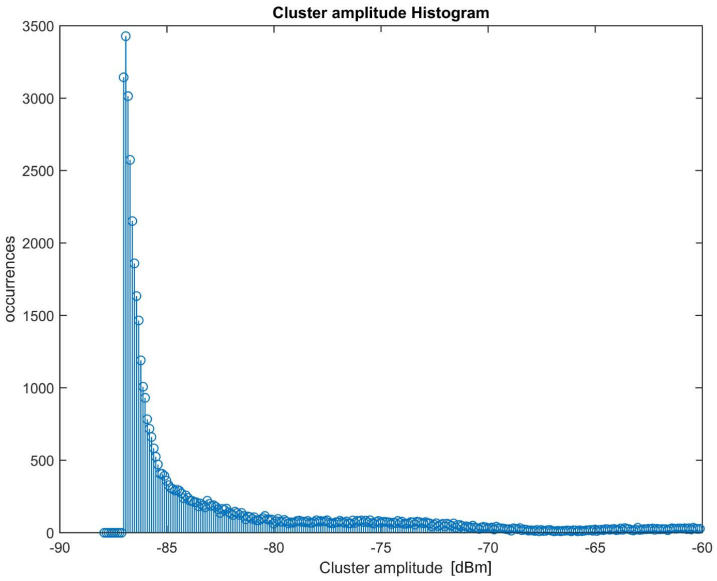

Figure 47. Oulu University Hospital, December, week measurements. WLAN Channel 6.

December data set, can be considered the "best" case. In fact, in this case, the cluster average amplitudes are low.

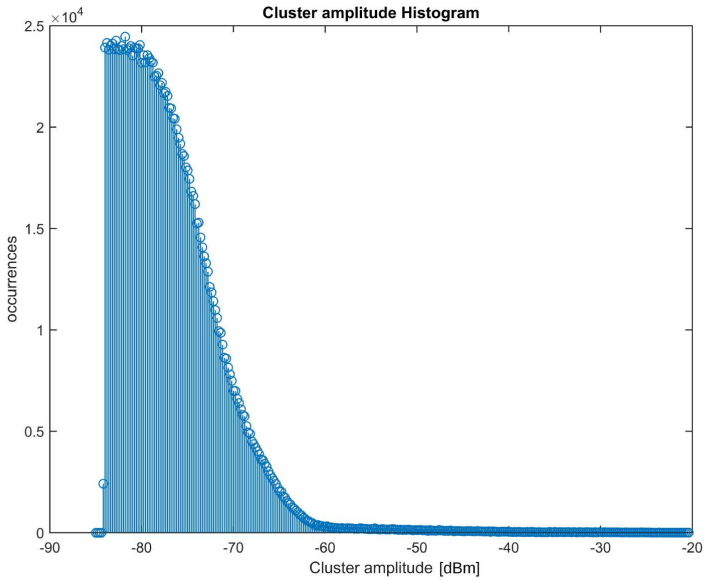

Figure 48. Oulu University Hospital, June, week measurements. WLAN Channel 1.

Figure 48 shows the cluster amplitude histogram achieved using June data set and WLAN channel 1 samples. The cluster's average amplitudes are in the range of -84÷-62 dBm (-84 dBm is the threshold). It is possible to compare the cluster amplitude histograms related to WLAN channel 1 samples, achieved using June and December data set. In Figure 48, the cluster average amplitudes assume values greater than in Figure 46. The most important difference between the occurrences shown in Figure 46 and Figure 48 is the number of clusters. In fact, WLAN channel 1 in June data set case presents a large amount of clusters. In Figure 48, the amplitudes closer to the threshold occur almost 25000 times. In Figure 46, the amplitudes closer to the threshold occur almost 6000 times.

WLAN channel 1, in June data set case, represents the "worst" case, in fact it presents a large amount of clusters. Moreover, these clusters have high average amplitude values and low discrete interarrival time values.

6.2. Interference modelling

In this section, the results shown in Section 6.1 are used to extract a statistical interference model, able to reproduce the interference behavior of the ISM band. The statistical model allows to represent the interference trend through statistical functions, such as CDF (cumulative distribution function) and PDF (probability density function), known in literature. The statistical model could be used to design the main parameters of a WBAN, in such a way that the WBAN could be immune to the interference modeled.

In this section, the CDFs related to clusters size, amplitude size and interarrival times vectors are calculated. These CDFs are called empirical CDFs. For each data set considered (i.e., December and June data set), 6 CDFs are computed (i.e., 3 CDFs related to WLAN channel 1 and 3 CDFs related to WLAN channel 6). Only the empirical CDFs related to the "best" case (i.e., WLAN channel 6, December data set) and the CDFs related to the "worst" case (i.e., WLAN channel 1, June data set) are reported. In this work, every empirical CDF is compared with 16 different CDFs, related to 16 different statistical distributions (statistical models), in order to identify the statistical distribution that best represents the empirical data. The most fitting statistical distribution is detected by using a Matlab script, called $allfitdist$ [44]. $allfitdist$ returns the best fitting distribution according to the Bayesian information criterion (BIC). The Bayesian information criterion selects the distribution that minimizes [30], [45]

$$BIC = -2 \cdot \ln(\hat{L}) + w \cdot \ln(v), \tag{15}$$

where v is the size of the vector achieved by data, i.e., cluster size, cluster amplitude or interarrival time vector size. w is the number of the parameters of the model considered, $\hat{L}$ is the maximized value of likelihood function for the statistical model considered, computed by [30], [45]

$$\hat{L} = p(y|\hat{\xi}, R), \tag{16}$$

where y is cluster size, cluster amplitude or interarrival time vector, $\hat{\xi}$ are the parameters, related to the model considered, that maximizes the likelihood function and R is the model considered [30], [45].

$allfitdist$ considers these distributions: Beta, Birnbaum-Sanders, Exponential, Extreme value, Gamma, Generalized extreme value, Generalized Pareto, Inverse Gaussian, Logistic, Log-logistic, Lognormal, Nakagami, Normal, Rayleigh, Rician, t location-scale and Weibull [39]. In every comparison, the Matlab script plots the empirical CDF and four CDFs, related to the four statistical distributions that best represent the empirical data, sorted from the best fitting distribution to the worst fitting distribution. $allfitdist$ represents also the CDF errors, i.e., the difference between the empirical CDF and every CDF related to these four statistical distributions.

6.2.1. Cluster size CDF

In this paragraph, the CDFs achieved using cluster size vector and the related calculated CDFs, are reported. In addition, errors based on the empirical and calculated CDFs are presented.

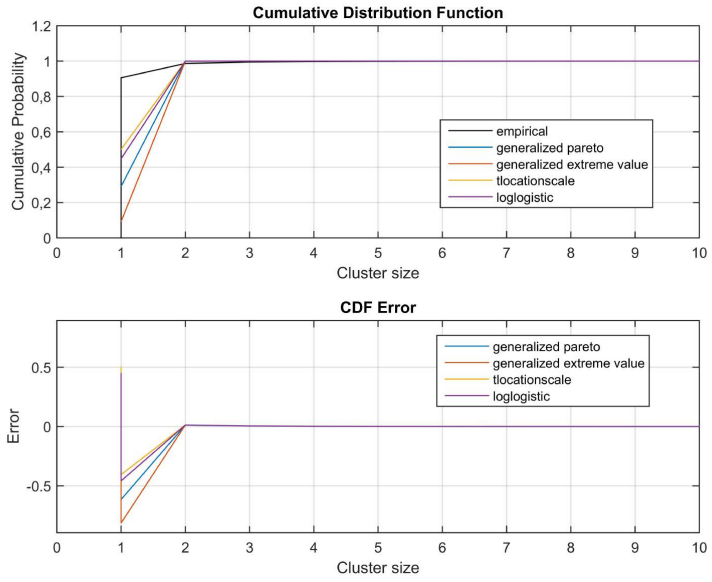

Figure 49. Oulu University Hospital, June, week measurements. WLAN Channel 1. On the top: Empirical and calculated CDFs of the cluster size. On the bottom: Calculated CDFs error.

Figure 49 shows that the empirical CDF (black line), related to the cluster size vector of the "worst" case assumes a value greater than 0.8 when a cluster size is equal to 1. This result is easily justifiable, in fact, as shown in Figure 43, the greatest number of clusters in WLAN channel 1 have a size equal to 1.

In this case, the empirical CDF is best represented by the Generalized Pareto distribution (blue line). The PDF related to Pareto distribution is computed by [46]

$$p(y|k,\sigma,\theta) = \frac{1}{\sigma} \cdot \left(1 + k \cdot \frac{(y-\theta)}{\sigma}\right)^{-1-\frac{1}{k}}, \tag{17}$$

for $\theta < y$, when $k > 0$, or for $\theta < y < \theta$-$\frac{\sigma}{k}$, when $k > 0$. k is the shape parameter, σ is the scale parameter and θ is the threshold parameter.

In this case, k = 4.8 , σ = 2.5e-15 and θ = 1. The other distributions, indicated in Figure 49, present a BIC higher than the BIC achieved with the Pareto distribution. The CDF error, shown in Figure 49, is remarkable for every distribution considered, mostly for low values of the clusters size. The CDF error is in the range -0.8÷-0.5.

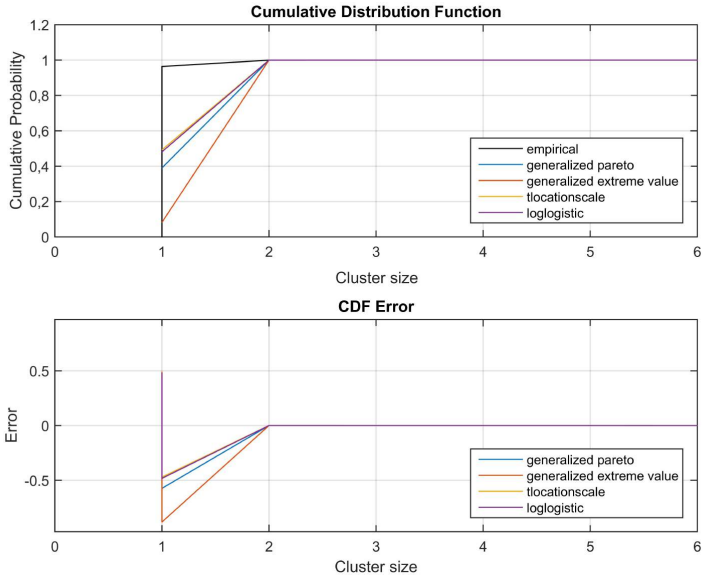

Figure 50. Oulu University Hospital, December, week measurements. WLAN Channel 6. On the top: Empirical and calculated CDFs of the cluster size. On the bottom: Calculated CDFs error.

Figure 50 shows an empirical CDF (black line) related to cluster size vector of the "best case" that is very similar to the empirical CDF in Figure 49. In fact, also in WLAN channel 6 (December data set), the greatest number of the clusters have a size equal to 1. In this case, the best fitting statistical distribution is the Pareto distribution (blue line), which PDF is indicated in (17). In this computation, k = 2.43 , σ = 2.34e-15 and θ = 1.

The CDF error, represented in Figure 50, is higher for the lowest values of the clusters size. The cluster size CDF error is the highest error achieved if compared with amplitude size and interarrival time CDF errors. This error is determined by the inability of the statistical distributions considered by the Matlab function $allfitdist$ to represent the particular shapes of the empirical cluster size CDF. For example, the empirical CDF shown in Figure 50 assumes a probability value equal to 0.9 as a function of a cluster size equal to 1. It means that 90% of the clusters, in this case, have a size equal to 1. The statistical distributions considered by $allfitdist$ are not able to model a so high value of probability as a function of a single value of cluster size, hence the cluster size CDF error is high.

6.2.2. Interarrival time CDF

This paragraph examines the empirical CDFs achieved using the interarrival time vectors and the related calculated CDFs. Also errors based on the empirical and calculated CDFs are reported.

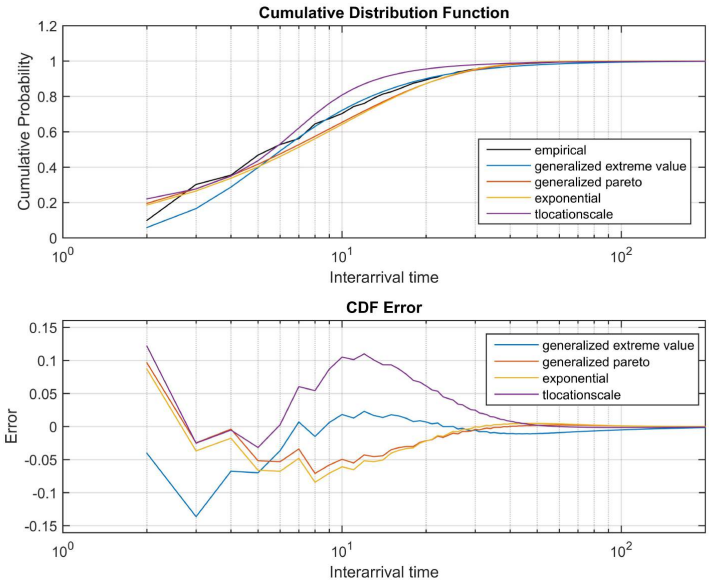

Figure 51. Oulu University Hospital, June, week measurements. WLAN Channel 1. On the top: Empirical and calculated CDFs of the interarrival time. On the bottom: Calculated CDFs error.

The empirical CDF (black line), related to interarrival time vector of the "worst" case, shown in Figure 51, reaches a value equal to 0.7 when an interarrival time is equal to 10 and a value equal to 0.9 when an interarrival time is equal to 20. It means that interarrival times greater than 20 are improbable. Figure 51 confirms that, as shown in Figure 44, WLAN channel 1 presents a continuous transmission.

Figure 51 indicates that the best fitting statistical distribution (blue line) is the Generalized extreme value (GEV). The PDF of GEV is computed by [47]

$$p(y|k,\mu,\theta) = \frac{1}{\sigma} \cdot \exp\left(-\left(1 + k \cdot \frac{(y-\mu)}{\sigma}\right)^{-\frac{1}{k}}\right) \cdot \left(1 + k \cdot \frac{(y-\mu)}{\sigma}\right)^{-1-\frac{1}{k}}, \quad (18)$$

for $1 + k \cdot \frac{(y-\mu)}{\sigma} > 0$. μ is the location parameter, σ is the scale parameter and k is the shape parameter. When $k > 0$ this distribution is called Frechet distribution. When $k < 0$ GEV corresponds to Weibull distribution [47]. In this case, k = 0.55, μ = 4.7, σ = 3.42. The CDF error, shown in Figure 51, is in the range -0.14÷0.12.

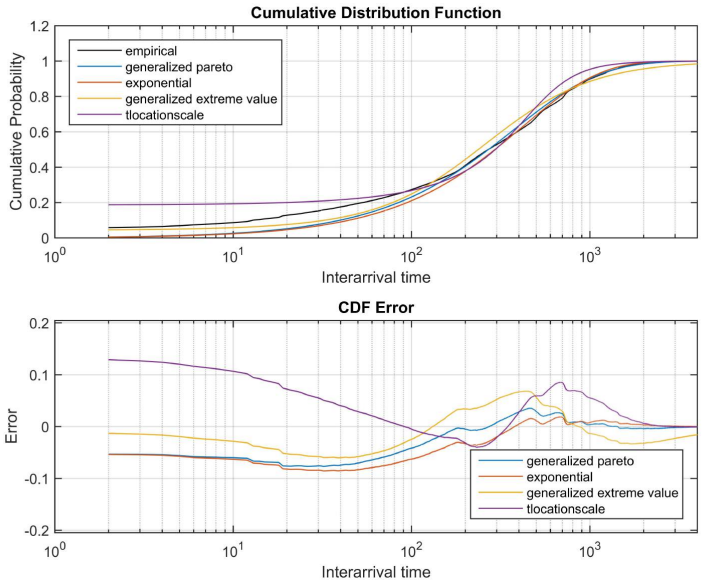

Figure 52. Oulu University Hospital, December, week measurements. WLAN Channel 6. On the top: Empirical and calculated CDFs of the interarrival time. On the bottom: Calculated CDFs error.

The empirical CDF (black line), related to the interarrival time vector, achieved with "best" case data, is shown in Figure 52. In this case, the empirical CDF reaches a value equal to 0.3 for an interarrival time value equal to 100. The empirical CDF is equal to 0.9 only for an interarrival time value equal to 1000.

The statistical distribution that best represents the empirical data is the Pareto distribution (blue line). The Pareto's PDF is shown in (17). In this case, k = 0.12, σ = 373.5 and θ = -2.2e-15. The CDF error, between the empirical CDF and every distribution represented, is in the range -0.1$\div$ 0.15.

6.2.3. Cluster amplitude CDF

In this paragraph the empirical CDFs achieved using the clusters amplitude vector and the related calculated CDFs, are examined. Also errors based on the empirical and calculated CDFs are presented.

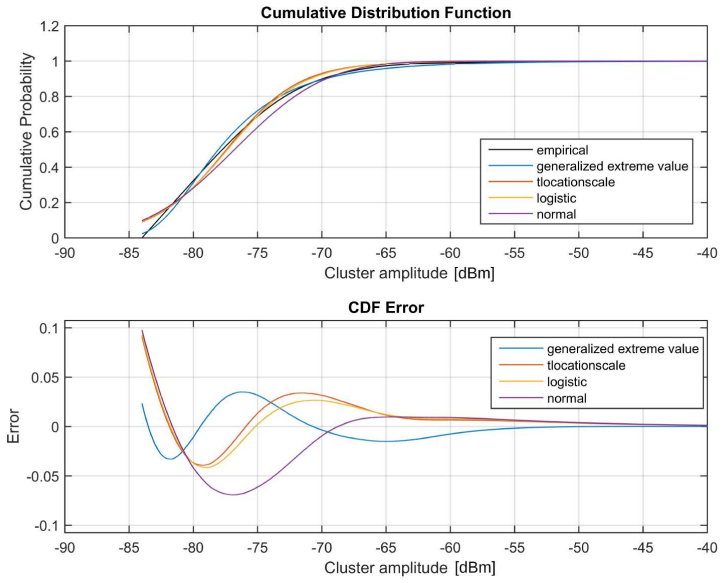

Figure 53. Oulu University Hospital, June, week measurements. WLAN Channel 1. On the top: Empirical and calculated CDFs of the cluster amplitude. On the bottom: Calculated CDFs error.

In Figure 53, the empirical CDF (black line) related to cluster size vector of the "worst case" assumes a value equal to 1 when a clusters average amplitude is equal to -60 dBm. This result is, obviously, in agreement with the results shown in Figure 48.

The distribution that best represents the empirical data is the Generalized extreme value distribution (blue line), which PDF is indicated in (18). In this case, k = 0.12, μ = -79.4, and σ = 3.7. The CDF error is in the range -0.07÷0.1, for every distribution represented.

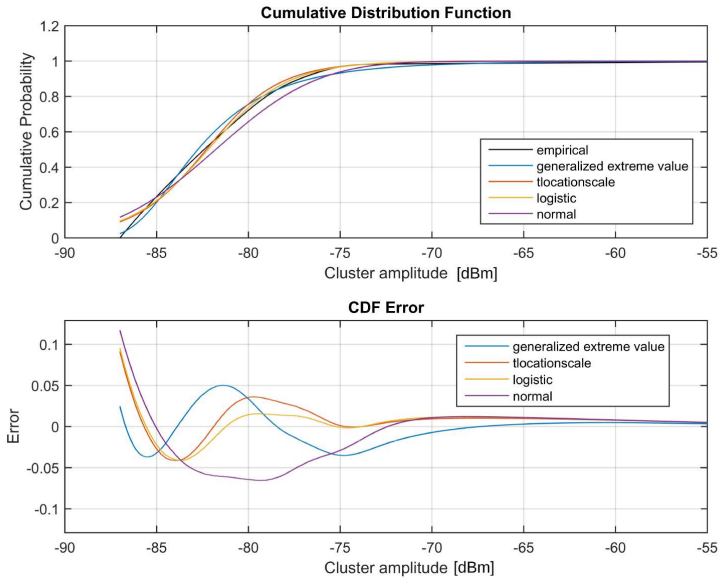

Figure 54. Oulu University Hospital, December, week measurements. WLAN Channel 6. On the top: Empirical and calculated CDFs of the cluster amplitude. On the bottom: Calculated CDFs error.

The empirical CDF (black line) related to the clusters amplitude vector, achieved using "best" case" data, is shown in Figure 54. In this case, the empirical CDF assumes a value equal to 1 when an amplitude value is almost -75 dBm.

The best fitting distribution is the Generalized extreme value (blue line), which PDF is shown in (18). In this case, k = 0.14, μ = -83.7, and σ = 2.7. The CDF error is in the range -0.06÷0.12.

7. DISCUSSION

The aim of this thesis was to carry out a time domain analysis and a spectrum occupancy evaluation of the ISM band, clustered around 2.4 GHz. Future WBAN, for healthcare applications, could use the ISM band, hence an aggregate interference evaluation in the ISM band is necessary. The analyses allow to understand if the ISM band still presents free spectrum resource for the implementation of a new WBAN or if it is too crowded to sustain a new network.

The analyses consider data collected in environments where a patient, monitored by WBAN sensor, could stay such as office, home and hospital. The analyses mostly focus on data collected in the hospital environment. In particular, these data was collected in the emergency ward of "San Giuseppe" hospital, located in Empoli, Italy and in Oulu University Hospital, situated in Oulu, Finland. In Oulu University Hospital, the first measurement campaign was carried out in December 2014, in the reception area at daily surgery building. The second measurement campaign was carried out in June 2014, in the accident and emergency ward.

The spectrum occupancy evaluation results strongly depend on the threshold, that can be fixed or dynamic. The analyses carried out considering the dynamic thresholds, evaluated using med-FCME algorithm, show results more accurate and precise than the results achieved using a fixed threshold. However, the algorithm used for evaluating the dynamic thresholds (i.e., med-FCME) is characterized by a high computational complexity and the computing time is considerable if compared with the algorithm based on a fixed threshold. An alternative algorithm able to exploit the speed and the simplicity of the algorithms based on a fixed threshold and the precision of the med-FCME has been proposed. In a future work, this algorithm could be implemented and tested considering data used in this work, in order to examine its performances and to compare them with the performances of med-FCME and the algorithm based on a fixed threshold.

The spectrum occupancy evaluation allows to compute FCO and FBO parameters. The results show that in office, home, "San Giuseppe" hospital and in the reception area at daily surgery building of Oulu University Hospital, the FCO is below 10% and the FBO is below 4%. Only the analysis carried out using data collected in the accident and emergency ward of Oulu University Hospital presents high FCO and FBO values. In this case, FCO values equal to 30% and FBO values of 13% are even reached.

The results of the analyses depend on the measurement location, the time and the measurement equipment. However, in most cases, the amount of interference in the ISM band is negligible and the implementation of a WBAN is possible. Despite the biggest number of analyses carried out in this work and in literature presented low values of occupancy, new measurement campaigns in strategic environments have to be carried out in order to understand if the results achieved using data collected in the accident and emergency ward of Oulu University Hospital, have to be considered an exception or a problem to evaluate.

A time domain analysis has been undertaken in order to examine the amplitude, the time distribution and the size of WLAN channel 1 and WLAN channel 6 clusters. The analyses were carried out considering data collected in the Oulu University Hospital measurement campaigns. The analyses show that WLAN channel 1 presents a large

amount of clusters. These clusters have high average amplitude values and low discrete interarrival time values. It means that the WLAN channel 1 transmission is almost continuous. The analyses show that WLAN channel 6 presents a little amount of clusters. These clusters have low average amplitude values and high interarrival time values. It means that the transmission is intermittent. In both WLAN channel 1 and WLAN channel 6, most of the clusters have a size equal to 1.

Due to this results, WLAN channel 1 was defined the "worst" case, WLAN channel 6 was defined the "best" case. The results achieved allow to extract an interference modelling, that represents the behavior of WLAN channel 1 and WLAN channel 6 clusters. In most cases, the statistical models that best represent both WLAN channel 1 and WLAN channel 6 are the Generalized Pareto and the Generalized extreme value distributions. In a future work, also other interference sources such as WLAN channel 11 can be modeled. Considering data collected in the accident and emergency ward of Oulu University Hospital it is possible to note a high occupancy value as a function of 2485 MHz. In a future work, this channel could be examined through a time domain analysis and modeled.

8. SUMMARY

The goal of this thesis was to survey the ISM band in order to understand how the radio spectrum related to ISM band is utilized and to know if there are still free spectrum resources that could be used for WBAN implementation. Time domain analyses and spectrum occupancy evaluation were carried out. Data used by the analyses was measured in strategic environments, where a patient, checked by WBAN sensors could spend most of his time, such as office, home and hospital environments.

After a concise introduction, an overview of WBAN and of the protocols that use the ISM band, such as WLAN, Bluetooth and Zigbee, is given. In particular, the features of PHY and MAC layer related to the protocols mentioned above are described. It is explained also that Bluetooth and Zigbee can support WBAN applications.

Next, the theoretical concepts related to the spectrum occupancy evaluation were reported. Moreover, the algorithms that allow to evaluate the occupancy are analyzed. The threshold used for evaluating the occupancy could be fixed or dynamic. The med-FCME algorithm, able to calculate the dynamic thresholds is minutely described.

Subsequently, the environments in which the measurement campaigns were carried out are described. In addition, the equipment and the measurement parameters used in every measurement campaign are examined. This information greatly influence the time domain analysis and the spectrum occupancy evaluation results.

The most important results of the spectrum occupancy evaluations are reported. The spectrum occupancy results are represented through graphics. These graphics depend on the environment, the measurement equipment and the threshold used, being either dynamic or fixed. The occupancy results achieved using every environment data are discussed and compared. The results achieved using dynamic thresholds are more accurate than the results derived using fixed threshold. Also the waterfall and percentile graphics are reported. These plots give important informations about the distribution of the power in the ISM band, but they are not connected to the problem of the spectrum occupancy evaluation.

Time domain analyses allow to know the amplitude, the time distribution and the size of the interference contributions. These informations are reported through the related histograms. These results allow to know the features, in time domain, of important interference sources, such as WLAN channel 1 and WLAN channel 6. WLAN channel 1 presents a continuous transmission. In this case the interference contributions assume high power amplitude. WLAN channel 6 is characterized by an intermittent transmission. The interference contributions related to WLAN channel 6 assume low power amplitude. The empirical CDFs, related to the time domain results are reported and compared with CDFs related to statistical models known in literature. The statistical distribution that best represent the interference behavior is identified. An interference model is achieved, removing the necessity of new measurement campaigns.

The results depend by the time, the measurement location and the measurement equipment, but in most cases the interference is not high, hence a WBAN implementation in the ISM band is possible.

9. REFERENCES

[1] ITU-R. (2011) ITU-R handbook spectrum monitoring.

[2] ITU-R SM.2256. 2012. Spectrum occupancy measurements and evaluation. Report, ITU-R.

[3] ITU-R SM.2180. 2010. Impact of ISM equipment on radio communications services. Report, ITU-R.

[4] Islam M., Koh C., Oh S.W., Qing X., Lai Y., Wang C., Liang Y.C., Toh B., Chin F., Tan G. & Toh W. Spectrum survey in Singapore: occupancy measurements and analyses. In: 3rd International Conference on Cognitive Radio Oriented Wireless Networks and Communications. CrownCom 2008. 15-17 May 2008, Singapore, pp. 1–7.

[5] Datla D., Wyglinski A.M. & Minden G. (2009) A spectrum surveying framework for dynamic spectrum access networks. IEEE Transactions on Vehicular Technology, vol. 58, pp. 4158–4168.

[6] Hoyhtya M., Lehtomaki J., Kokkoniemi J., Matinmikko M. & Mammela A. Measurements and analysis of spectrum occupancy with several bandwidths. In: IEEE International Conference on Communications (ICC), 9-13 June 2013, Budapest, Hungary, pp. 4682–4686.

[7] Lopez-Benitez M. & Casadevall F. On the spectrum occupancy perception of cognitive radio terminals in realistic scenarios. In: 2nd International Workshop on Cognitive Information Processing (CIP), 14-16 June 2010, Elba, Italy, pp. 99–104.

[8] Biggs M., Henley A. & Clarkson T. (2004) Occupancy analysis of the 2.4 GHz ISM band. IEE Proceedings Communications, vol. 151, pp. 481–488.

[9] Denkovski D., Pavloski M., Atanasovski V. & Gavrilovska L. Parameter settings for 2.4 GHz ISM spectrum measurements. In: 3rd International Symposium on Applied Sciences in Biomedical and Communication Technologies (ISABEL), 7-10 Nov 2010, Rome, Italy, pp. 1–5.

[10] Kokkoniemi J. & Lehtomaki J. Spectrum occupancy measurements and analysis methods on the 2.45 GHz ISM band. In: 7th International ICST Conference on Cognitive Radio Oriented Wireless Networks and Communications (CROWNCOM), 18-20 June 2012, Stockholm, Sweden, pp. 285–290.

[11] Lehtomäki J.J., Vuohtoniemi R., Umebayashi K. & Mäkelä J. (2012) Energy detection based estimation of channel occupancy rate with adaptive noise estimation. IEICE Transactions, vol. 95-B, pp. 1076–1084.

[12] Ghosh C., Pagadarai S., Agrawal D. & Wyglinski A.M. (2010) A framework for statistical wireless spectrum occupancy modeling. IEEE Transactions on Wireless Communications, vol. 9, pp. 38–44.

[13] Gibson A. & Arnett L. Measurements and statistical modelling of spectrum occupancy. In: Sixth International Conference on HF Radio Systems and Techniques, 4-7 July 1994, York, United Kingdom, pp. 150–154.

[14] Wang Z. & Salous S. (2011) Spectrum occupancy statistics and time series models for cognitive radio. J. Signal Process. Syst., vol. 62, pp. 145–155. URL: http://dx.doi.org/10.1007/s11265-009-0352-5.

[15] Wellens M., de Baynast A. & Mahonen P. (2008) Performance of dynamic spectrum access based on spectrum occupancy statistics. IET Communications, vol. 2, pp. 772–782.

[16] Stabellini L. Quantifying and modeling spectrum opportunities in a real wireless environment. In: IEEE Wireless Communications and Networking Conference (WCNC), 18-21 Apr 2010, Sydney, Australia, pp. 1–6.

[17] Pierucci L. WLAN. IEEE 802.11 family. Lecture notes, University of Florence.

[18] Virk M.H., Vuohtoniemi R., Hämäläinen M., Mäkelä J.P. & Iinatti J. Spectrum occupancy evaluations at 2.35-2.50 GHz ISM band in a hospital environment. In: 9th International Conference on Body Area Networks, BodyNets '14, Sept 29-Oct 1 2014, London, United Kingdom, pp. 39–45. URL: http://dx.doi.org/10.4108/icst.bodynets.2014.256965.

[19] Virk M.H. (2013) Design and implementation of a multi-purpose wireless body area network. Master's thesis, University of Oulu.

[20] Collodi G. Technologies and Systems for Wireless applications. Lecture number 3. University of Florence.

[21] Chen M., Gonzalez S., Vasilakos A., Cao H. & Leung V. (2011) Body area networks: A survey. Mobile Networks and Applications, vol. 16, pp. 171–193. URL: http://dx.doi.org/10.1007/s11036-010-0260-8.

[22] Bilstrup K. (2008) A preliminary study of WBAN. Technical report IDE0854, Halmstad University.

[23] List of WLAN channels (site visited on 25-2-2015) URL: http://en.wikipedia.org/wiki/List-of-WLAN-channels.

[24] Wireless LAN networking, white paper (site visited 20-2-2015) URL: http://support.usr.com/download/whitepapers/wireless-wp.pdf.

[25] Muller N. (2001) Bluetooth Demystified. Demystified Series, McGraw-Hill. URL: http://books.google.fi/books?id=9v1SAAAAMAAJ.

[26] Pierucci L. Bluetooth. Lecture notes, University of Florence.

[27] Bluetooth: Overview of architecture, PHY and MAC (site visited on 25-2-2014) http://www.cs.tut.fi/kurssit/TLT-6556/Slides/2-Bluetooth.pdf.

[28] Niemelä V. (2010) Low-complexity ultra wideband receivers in medical applications. Master's thesis, University of Oulu.

[29] Pierucci L. Wireless sensor network. Lecture notes, University of Florence.

[30] (2013-2012) Smart body area networks (SMARTBAN); Coexistence. Technical report, ETSI.

[31] Yucek T. & Arslan H. Spectrum characterization for opportunistic cognitive radio systems. In: IEEE Military Communications Conference. MILCOM 2006. 23-25 Oct 2006, Washington, DC, pp. 1–6.

[32] Vartiainen J., Saarnisaari H., Lehtomaki J. & Juntti M. A blind signal localization and SNR estimation method. In: IEEE Military Communications Conference, 2006. MILCOM 2006. 23-25 Oct 2006, Washington, DC, pp. 1–7.

[33] Vartiainen J. (2010) Concentrated signal extraction using consecutive mean excision algorithms. Doctoral dissertation, University of Oulu.

[34] Vartiainen J., Lehtomaki J. & Saarnisaari H. Double-threshold based narrowband signal extraction. In: IEEE 61st Vehicular Technology Conference, VTC 2005-Spring, May 30-June 1 2005, vol. 2, pp. 1288–1292.

[35] Matinmikko M. (2012) Spectrum sharing using cognitive radio system capabilities: methods to obtain and exploit knowledge of spectrum availability. Tech. rep., VTT.

[36] Matinmikko M., Mustonen M., Höyhtyä M., Rauma T., Sarvanko H. & Mämmelä A. Distributed and directional spectrum occupancy measurements in the 2.4 GHz ISM band. In: 7th International Symposium on Wireless Communication Systems. ISWCS 2010. 19-22 Sept 2010, University of York, York, United Kingdom.

[37] Wellens M. & Mahonen P. Lessons learned from an extensive spectrum occupancy measurement campaign and a stochastic duty cycle model. In: 5th International Conference on Testbeds and Research Infrastructures for the Development of Networks Communities and Workshops. TridentCom 2009. 6-8 Apr 2009, Washington, DC, pp. 1–9.

[38] Mucchi L., Carpini A., Kumpuniemi T., Hamalainen M. & Iinatti J. Evaluation of the aggregate interference in hospital ISM band. In: 9th International Conference on Body Area Networks, BodyNets '14, Sept 29-Oct 1 2014, London, United Kingdom.

[39] Mucchi L. & Carpini A. ISM band aggregate interference in BAN-working environments. In: 8th International Symposium on Medical Information and Communication Technology (ISMICT), 2-4 Apr 2014, Florence, Italy, pp. 1–5.

[40] Mucchi L., Carpini A., D'Anna T., Virk M.H., Vuohtoniemi R., Hämäläinen M. & Iinatti J. Threshold setting for the evaluation of the aggregate interference in

ISM band in hospital environments. In: 9th International Symposium on Medical Information and Communication Technology (ISMICT), 24-26 Mar 2015, Kamakura, Japan, pp. 1–5.

[41] RF Explorer model 2.4 G (site visited on 11-3-2015) URL: http://www.seeedstudio.com/depot/RF-Explorer-model-24G-p-924.html.

[42] Mucchi L., Trippi F., Carpini A. & Amato M. Performance of wireless ECG monitoring in city hospital in the presence of interference. In: 7th International Conference on Body Area Networks, BodyNets '12, 24-26 Sept 2012, Oslo, Norway, pp. 230–234. URL: http://dl.acm.org/citation.cfm?id=2442691.2442745.

[43] Mucchi L., Trippi F., Carpini A., Amato M. & Cozzani R. Performance of wireless real-time system for ECG monitoring in hospitals. In: 6th International Symposium on Medical Information and Communication Technology (ISMICT), 25-29 Mar 2012, San Diego, California, pp. 1–5.

[44] ALLFITDIST fit all valid parametric probability distributions to data, (site visited on 27-02-2015) URL: http://www.mathworks.com/matlabcentral/fileexchange/34943-fit-all-valid-parametric-probability-distributions-to-data.

[45] Stoica P. & Selen Y. (2004) Model-order selection: a review of information criterion rules. IEEE Signal Processing Magazine, vol. 21, pp. 36–47.

[46] Generalized Pareto Distribution, (site visited on 4-03-2015) URL: http://se.mathworks.com/help/stats/generalized-pareto-distribution.html.

[47] Generalized Extreme Value Distribution, (site visited on 4-3-2015) URL: http://se.mathworks.com/help/stats/generalized-extreme-value-distribution.html.